2011

Foldable substrates for micro-ultrasonic transducers

Karthik Balasubramanian
Louisiana State University and Agricultural and Mechanical College

FOLDABLE SUBSTRATES FOR MICRO-ULTRASONIC TRANSDUCERS

A Thesis

Submitted to the graduate faculty of the
Louisiana State University and
Agricultural and Mechanical College
In partial fulfillment of the
Requirements for the degree of
Master of Science in Electrical Engineering

in

The Department of Electrical and Computer Engineering

By
Karthik Balasubramanian
B.E, Anna University, India, 2008
December 2011

ACKNOWLEDGEMENTS

First and foremost, I would like to express my sincere gratitude to my advisor, Dr. Dooyoung Hah for his invaluable support, encouragement, guidance and inspiration he gave for the successful completion of my thesis.

I would also like to thank Dr. Martin Feldman and Dr. Theda Daniels-Race for being a part of my committee.

A special thanks to Mr. Golden Hwaung for training me to use the equipments and also helping me in learn new things. I am also grateful to my fellow students and friends Anirban, Ragav, Pradeep, Dan and Pallavi for lending their help and suggestions whenever needed.

I would also like to thank Kang for training and helping me to conduct my experiments at CAMD. Also I am grateful to all my friends out here at Baton Rouge for making my time enjoyable here at LSU.

Finally I would like to thank my parents and brother for their unconditional love and support throughout these years. Above all I would like to thank God, who has been my marshal and light all these years and will be in future.

TABLE OF CONTENTS

LIST OF TABLES

LIST OF FIGURES

ABSTRACT

Ultrasound has broad range of applications from underwater examination, nondestructive testing of materials and medical diagnosis and treatment. The ultrasonic transducer plays an vital role in determining the resolution, sensitivity, as well as other diagnostic capabilities of an ultrasonic imaging system. Current piezoelectric transducer which dominates the medical field has limited applications compared to the capacitive ultrasonic transducer. The capacitive transducer is easy to fabricate compared to the piezoelectric transducer.

In this work, the fabrication of a foldable substrate for a capacitive ultrasonic transducer has been discussed. The foldable substrate was fabricated using an ultrathin silicon wafer which is 50 µm thick by using the principle of polymer shrinkage. It is believed that the foldable substrate can be used in intravascular ultrasound (IVUS) and endoscopic ultrasound (EUS) applications for next generation biomedical imaging.

1. INTRODUCTION

Ultrasound refers to cyclic sound pressure with a frequency greater than 20 kHz. It has wide variety of application starting from industrial testing, therapeutic healthcare, etc. The use of ultrasound for biomedical imaging is very safe and has no adverse health effects as it does not use any ionizing radiation.

1.1 Ultrasonography.

The diagnostic imaging method in which ultrasound waves are used to visualize a deep internal body structure which includes muscles, joints or organs is called as ultrasonography. This is also called as sonography or echography. This is also known as echocardiography when used in imaging and treatment of heart diseases.

Medical ultrasonography was invented by cardiologist Inge Edler and Hellmuth Hertz [1]. A regular ultrasonography uses sound waves between 1 MHz and 20 MHz [2]. The history of ultrasonography dates back to 1880 with the discovery of piezoelectric effect by Pierre Curie. Later during the World War I, the SONAR (SOund Navigation And Ranging) was developed as a detection system for underwater navigation. The high frequency ultrasonic submarine detector was invented by P. Langevin in the year 1917. Since then the ultrasound had been largely used in industries and defense purpose [3]. The first application of ultrasound in medical field was for the imaging of brain tumor [4]. Earlier ultrasound was mainly used in pregnancies but lately, they are being used in many other parts of the body as well. Ultrasonography is not only used for diagnostics but also for treatment and prevention of many severe medical conditions. Since late 1970s the ultrasound has been regularly used in the medical industry. The standard ultrasound is the one which has 2-D imaging and it is widely

used. Sometimes due to medical complications, there arises a situation where 2-D image does not provide enough information and also it is difficult to visualize and transform a series of 2-D images into a 3-D one. In such cases, 3-D image of ultrasound can be used. There has been much research going on in 3-D ultrasonography from middle 1990's [5]. The more recent advancement in the ultrasonography is the 4-D imaging which is similar to 3-D imaging but with moving pictures [6].

1.2 Typical Ultrasonic Imaging System

The basic block diagram of the system is shown in figure 1.1. An ultrasonic system usually has 3 main parts. They are:

1. Transducer arrays
2. Processing unit and
3. Image reconstruction unit.

The processing unit contains transmitter pulsar, low noise amplifier (LNA), time gain controlled (TGC) amplifier, a low pass filter and analog to digital converter (ADC). The image reconstruction unit contains image processing electronics and displays. [8]

Under normal operating conditions the transducer acts as both transmitter and receiver. The signals that are reflected are detected by the receiver and processed as electrical signals and the image is reconstructed. The main performance determining factor in an ultrasound system is the quality of echoed and reflected signals from the tissues, thus making transducer a really essential part of an ultrasonography.

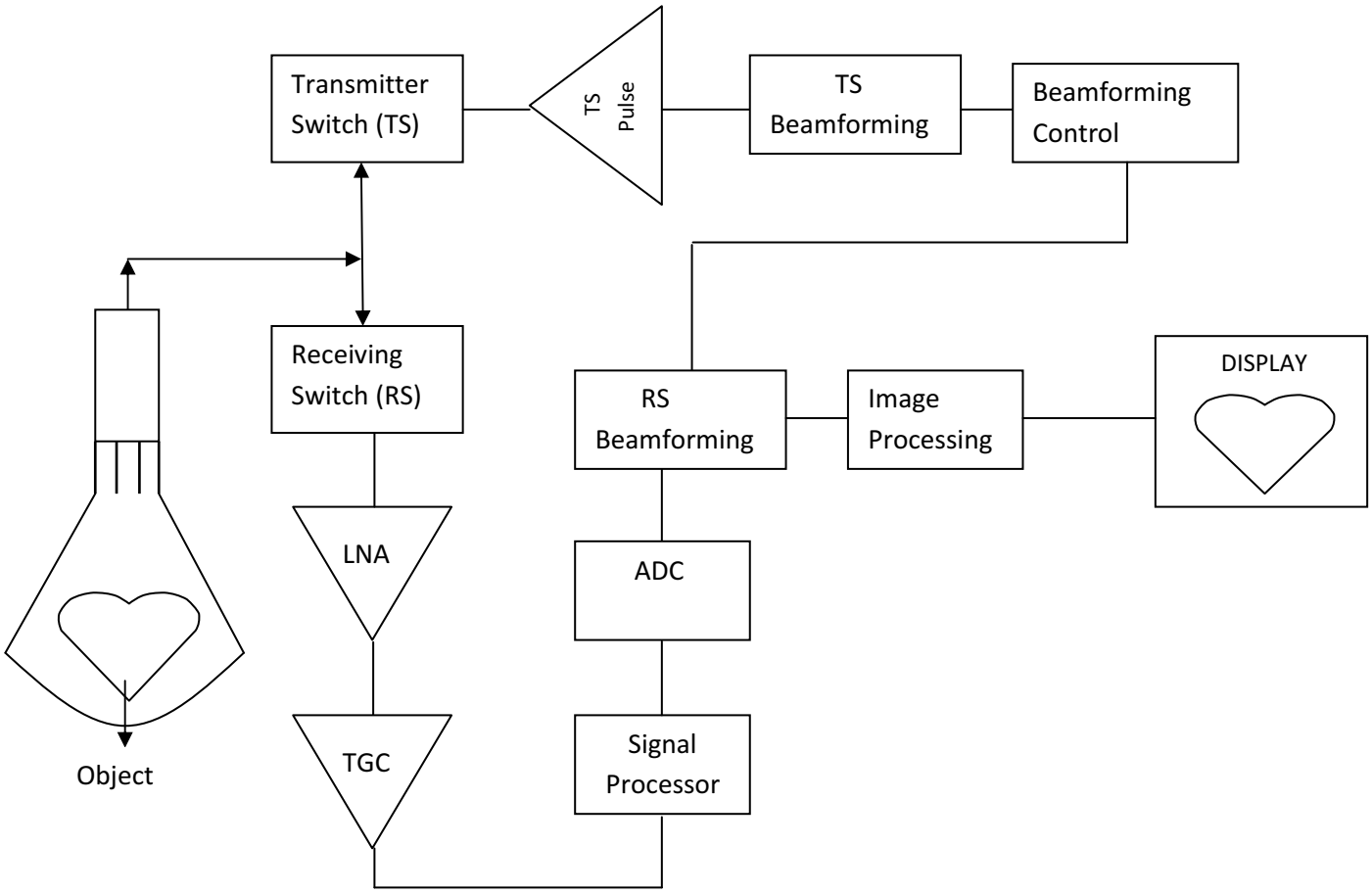

Figure 1.1: Block diagram of an ultrasonography.

1.3 Ultrasonic Wave Propagation in Media

The basic idea of an ultrasonography is to send ultrasound waves into the body or object and the waves are reflected back at the interface with tissue or any surface. The depth of the flaw (defects) or the reflecting tissue is determined by the return time of the ultrasound waves. The image quality depends upon the quality and clarity of the reflected wave. Thus it has become essential to study the propagation of ultrasonic waves.

In general, sound waves can travel in four different modes. They are

1. Longitudinal waves,
2. Shear (transverse) waves,
3. Surface waves and
4. Plate waves.

Longitudinal and transverse waves are the two most common modes of wave propagation used in ultrasound. In longitudinal waves, the sound particles move in parallel to the direction of propagation of the waves. The sound particles in the longitudinal waves oscillate back and forth in their medium. The longitudinal waves are also called as the compressional or pressure waves. In transverse waves, the sound particles move perpendicular to the wave propagation direction. In medical applications, longitudinal waves are most commonly used as it can be more easily penetrated. Transverse waves propagate only in solid bodies.

Once the ultrasonic waves are transmitted, they hit the target and reflect back. These reflected echoes determine the quality of the image obtained and are mostly of two types. They are

1. **Specular Echoes**. These are echoes that originate from a flat regular shaped object. These are generally angle dependent and intense.

2. **Scattered Echoes.** These echoes originate from small irregular shaped objects. These are less intense and are not angle dependent.

1.3.1 Ultrasound Wave Propagation

The basic propagation of an ultrasound waves inside a medium is shown in figure 1.2. We can see that the beam patterns have two regions. They are Fresnel and Fraunhofer regions. The beam pattern changes as one move from Fresnel to Fraunhofer zone. The beam pattern in Fresnel and Fraunhofer region is shown in fugure 1.3. From the figure 1.3, we can see that the wave propagation depends mainly on the source diameter and also the wavelength of the wave. More details about this will be in chapter 2.

1.3.2 Resolution and Depth of Penetration

The wavelength and frequency in an ultrasonic wave is given by the relation [9].

$$V = n \lambda$$

Where, V= propagation velocity of sound.

n= frequency

λ= wavelength

Deciding the frequency in which the transducer should operate is the key. From the above equation, we can see that for a constant sound velocity, by changing the frequency, the wavelength also changes. The wavelength determines the resolution of the image and depth of penetration. The general rule of thumb is as follows.

When frequency increases, the wavelength decreases, resolution increases and the depth of penetration of ultrasound decreases and vice versa. Also**,** as the frequency increases the beam divergence decreases, i.e. for high frequencies there is narrow beam width.

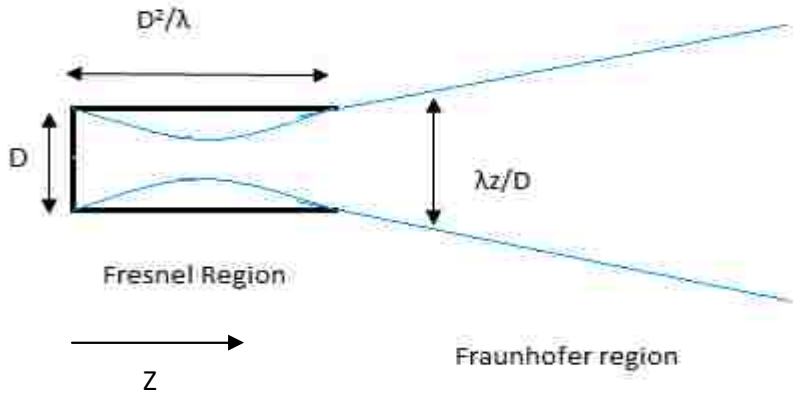

Figure 1.2: Propagation of an ultrasound waves. λ: wavelength

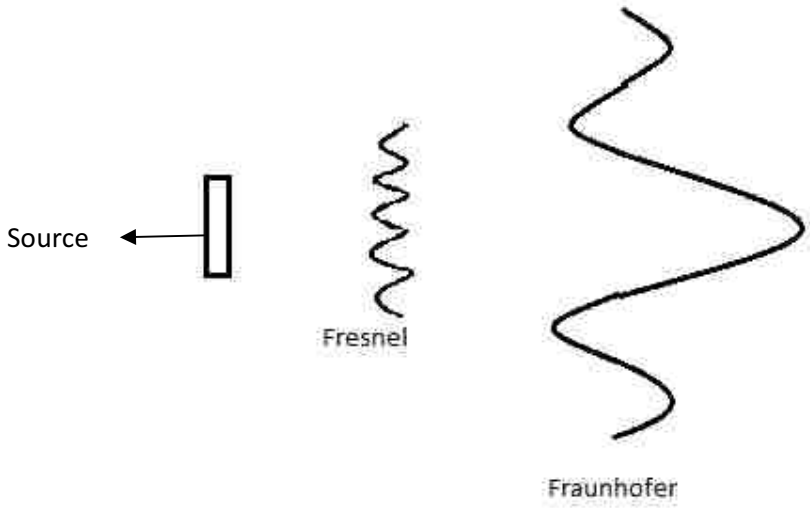

Figure 1.3: Beam pattern formation in different regions

Generally for medical applications the desired frequency is between 1 and 20 MHz. A recent study of nearly 35 patients who were suffering from melano cytama, the frequencies of the ultrasound used was 20 MHz. This study was done to demonstrate the use and advantages of high resolution ultrasound. The final results show that the high resolution ultrasound enabled enhanced accuracy for the detection of the lesion dimension and the growth and malignant transformation was documented more accurately [10]. Although there are many studies which show the advantages of high frequency ultrasound, the tradeoff between the resolution and penetration depth limits its usage [11]. For areas such as eyes where the depth is very low, high frequency ultrasound is used where as in parts where the depth of penetration is more, low frequencies are used. Table 1.1 show the human parts and the corresponding frequency of ultrasound (c= 1500m/s). For high resolution imaging of inner bodies, advanced methods such as endoscopic ultrasonography (EUS) and intravascular ultrasonography (IVUS) were developed.

Table 1.1: Commonly used frequencies and its corresponding wavelength in different areas

Application	**Frequency**	**Wavelength**
Fetus in pregnant women	1 MHz	1.5 mm
Eye	10 MHz	0.15 mm
Skin	20 MHz	0.075 mm

1.3.3 Acoustic Impedance and Impedance Mismatch

Acoustic impedance, also known as the sound impedance is a parameter which depends on frequency. It is the ratio between the acoustic pressure to acoustic volume flow. It is given by,

$$\text{Acoustic impedance } (Z) = p/U$$

Where, p= sound pressure

U= volume flow

Characteristic acoustic impedance sometimes referred to as characteristic impedance of an medium is the product of the density of that medium and the velocity of sound in that medium.

$$\text{Characteristic acoustic impedance } (Z_0) = \rho V$$

Where, ρ = density of the medium

V = velocity of sound in the medium.

The characteristic impedance is a very important feature to be kept in mind while designing an transducer. The characteristic impedance is essential in

i. Determination of degree of reflection and refraction at the boundary of two material where there is impedance mismatch.
ii. Absorption of sound in medium. [12]

For most of the biological materials in tissue, the value of characteristic acoustic impedance (Z_0) is 1.6×10^5 g/ (Cm^2.S) approximately. Whenever an ultrasonic wave comes across the change in layer or the interface of two layers then there is both reflection and refraction of the

ultrasound. Greater the impedance mismatch between layers, greater the reflection of the ultrasound waves. Table 1.2 shows the characteristic impedance for some materials.

Table 1.2: Characteristic impedance of selected materials

Material	**Characteristic impedance [g/ (Cm^2.S)] * 10^5**
Air	0.0004
Water	1.5
Aluminum	17
Blood, kidney, liver, etc.	1.5 - 1.7
Oil	1.4

The amount of wave reflected is given by the equation 2.

$$[(Z1 - Z2)/(Z1 + Z2)]^2$$

Where Z_1 = impedance of the layer 1

Z_2 = impedance of the layer 2

The most common impedance mismatch issue in the medical ultrasonography is that between the air and the human tissue. The characteristic acoustic impedance of air is 42.8 g/ (cm^2.s) and that of the tissue is $1.6x10^5$ g/ (cm^2.s). The mismatch is so large that almost 99% of the ultrasound is reflected back. In order to prevent this from happening an impedance matching layer is usually used. The common matching layers used in medical ultrasonogrphy are olive oil or jelly. Figure 1.4 shows the use of matching layer so that the air is eliminated between the transducer and tissue. Here, Z_m is the impedance of the matching layer.

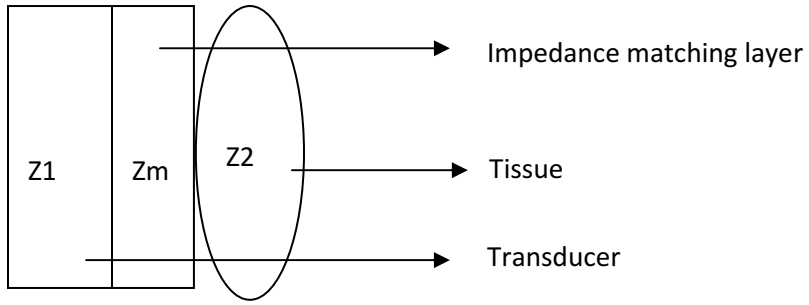

Figure 1.4: Impedance matching layer to minimize reflection.

By using this method, almost 70-80% of the waves are transmitted and the rest is reflected back.

1.4 Endoscopic Ultrasonography (EUS) and Intravascular Ultrasonography (IVUS)

Endoscopic Ultrasonography (EUS)

This is an imaging technique which combines the concept of endoscopy and ultrasonography. In general endoscopy refers to insertion of a long flexible tube like structure to diagnose gastrointestinal and lung disease. The tubes are generally inserted either through mouth or rectum. The main advantage of a EUS is that it has high quality image compared to the traditional ultrasound due to the proximity of the transducer to the target organs. EUS can also be used in the study of blood flow inside the vessels using dopler ultrasound [13]. Since EUS is done from inside the body, touching the target area it takes a longer time compared to the traditional transducer but it gives a lot of details about the disease. Although there are many advantages of using EUS, it also has a few disadvantages. There is a possibility that the patient might develop hives, skin rash, etc. The biggest disadvantage of using the EUS is that there is a possibility of perforation, i.e. making a hole in the wall of the intestine. Although

these are serious issues, the chance of happening is less than 1%. There are enough precautions that can prevent it.

IVUS

IVUS is also an ultrasonic imaging technique which is very unique and allows in-vivo imaging of individual vessels. It is used in imaging of the cross section view of the blood vessels from inside out [14]. This gives a very unique point-of-view picture that is generated in real time. IVUS uses a specially designed catheter (a tube that can be inserted inside the body) and has a transducer at the tip of the catheter. In IVUS, the image shows the distinctive circular layers of coronary arteries.

The main advantage of IVUS compared to angiogram (an X-Ray test) is that it uses cross section view of the human body instead of the side view. Also angiography has the limitation to access coronary disease. In an angiogram, only one section of lumen can be scanned, whereas in IVUS the vessel wall and lumen visualization can be seen. Figure 1.5 shows the main imaging differences between angiogram and IVUS. The arrows suggest the imaging direction.

1.4.1 Modes of Operation

As mentioned in the previous section the IVUS utilizes a long flexible tube called catheter and this supports the imaging probe at the tip. This probe has the transducer elements mounted on it. This imaging probe receives and transmits ultrasound signal. The transducer is placed on the tip of the probe and determines the modes of operation.

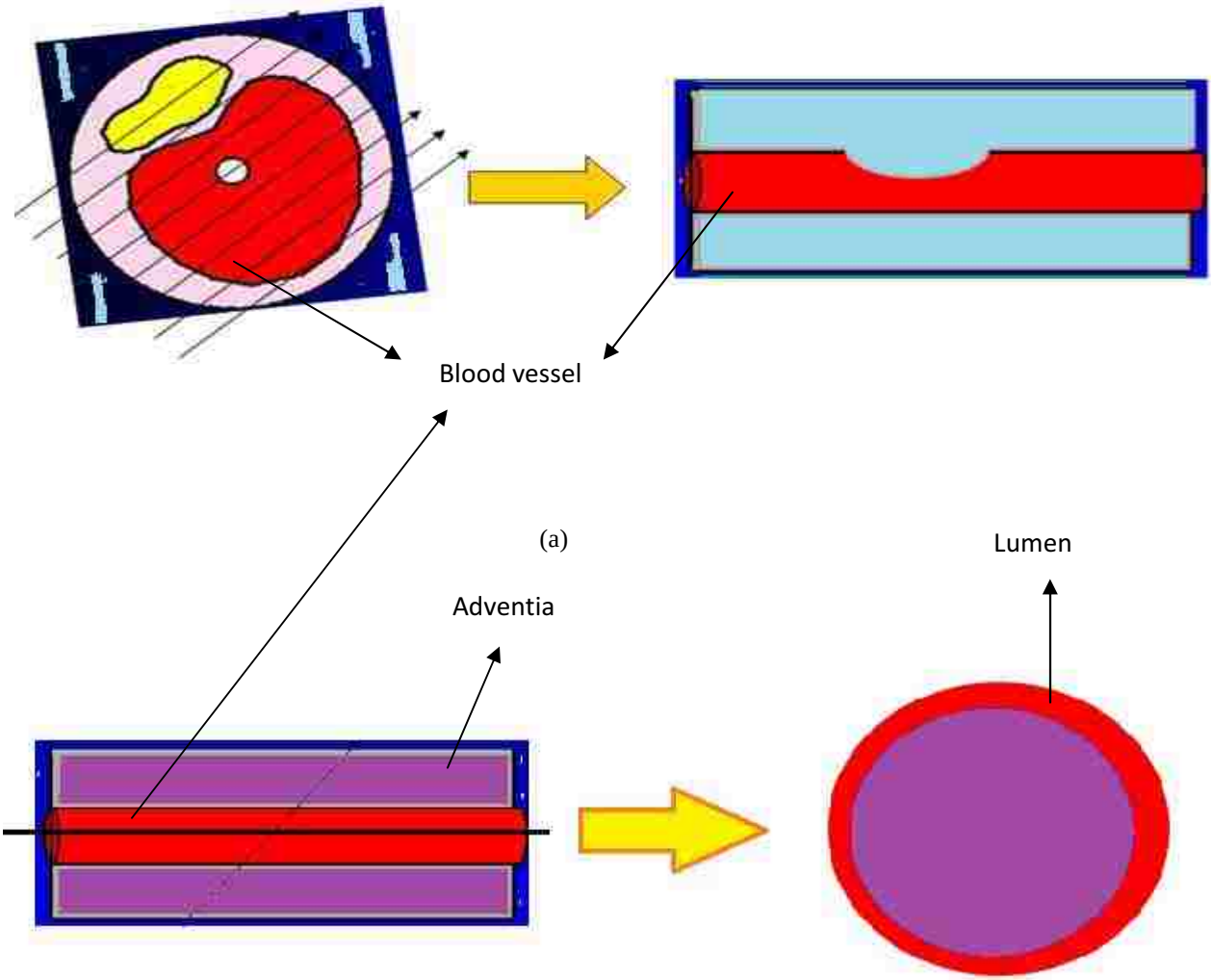

Figure 1.5: (a) Angiogram versus (b) IVUS

There are three main modes of operation. They are

- Forward Looking
- Side Looking
- Combination

Based on the locations of the transducers, the ultrasonography can be either forward or side looking. The forward looking ultrasound system was put into practice by using annular arrays mounted on the front end of the catheter [15-16]. But these transducers have limited side viewing angle. There are also side looking transducers which image the side tissue. There can be either single transducer which is rotated mechanically or else there can be array of transducers. There also exists multi-looking IVUS [17-18] in which transducer is divided into two sections. Longer section is mounted on the sidewall to be side looking and the shorter end is bent to be in the front end as a forward looking. By this method of mounting, the real time 3-D imaging is possible. Figure 1.6 shows the model of the transducer mounted on the probe which is forward and side looking.

1.4.2 Need of Foldable Substrate

For some applications, a flexible or foldable substrate is necessary. There are situations where the capacitive transducers need to be placed on the non flat surfaces and in such case it is necessary to have a foldable substrate. Earlier in the piezoelectric transducers, the individual elements were cut and placed on a foldable substrate manually. The main drawback here is that individual elements are not fabricated in the substrate itself. Fabricating the device on the foldable substrate is the advantage of using capacitive micromachined ultrasonic transducer (CMUT). This will be mainly used in medical applications. For example in EUS and IVUS, a small transducer element is placed on the tip of a catheter and inserted into the human body.

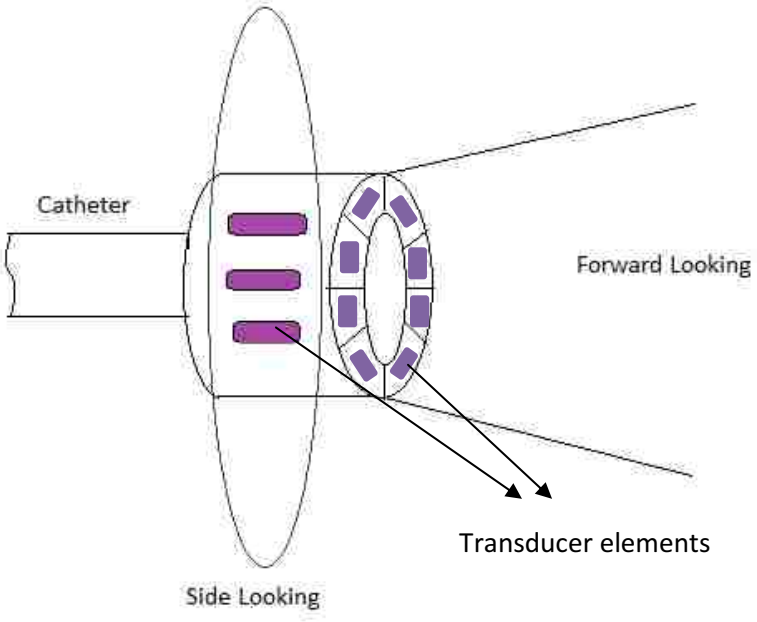

Figure 1.6: Multi-looking ultrasonic probe.

For such applications, it is necessary to have folding mechanism. Although there have been few transducers whose substrates are folded but, the main issue is their substrates cannot be controlled or changed once it has been folded. The flexible substrates have the advantage of light weight, robust and absorb stress better than the conventional one. More details about the foldable substrate will be provided in chapter 3.

1.5 Micro-ultrasonic Transducers

In general, a transducer is a device that converts one type of energy into another. Traditionally, piezoelectric material was used for ultrasonic transducer. Piezoelectric material can efficiently convert the electrical pulse into mechanical vibration and vice versa. The basic concept of piezoelectricity is that it produces an electrical field when the mechanical stress is applied and a mechanical vibration if an electrical field is applied. The piezoelectric

effect was first discovered by the Curie brothers in 1880. The two materials that were very helpful for the ultrasound production are piezoelectric polymers and Ceramics. The details about the polymers and the ceramics can be found in [19]. The most important type of the piezoelectric ceramic is the lead zirconate-titanate also known as PZT. The main advantage of this PZT is that it has high piezoelectric coefficient [20]. The acoustic impedance of a piezoelectric material is almost same as the solid metal which leads in the impedance mismatch of the transducer with tissue, which is a serious drawback of the piezoelectric ultrasonic transducer. This has led to the new type of transducer called as the capacitive micromachined ultrasonic transducer (CMUT). The basic principle and the introduction of the CMUT will be detailed in chapter 2.

1.6 Organization of Thesis

Chapter 2 starts with the introduction about the capacitive type transducer, operation principle, design parameters of the transducer and the ANSYS simulation for the resonant frequency study.

Chapter 3 will focus on the foldable substrate of the transducer. Design details for the silicon foldable substrate will be presented along with the process flow and the results.

Chapter 4 will focus on conclusions and the future work.

2. DESIGN OF CAPACITIVE MICRO-ULTRASONIC TRANSDUCERS

2.1 Preamble

In this chapter the main emphasis will be on capacitive micromachined-ultrasonic transducer (CMUT). These are very tiny transducers that will be replacing the conventional piezoelectric transducers for imaging and blood flow monitoring applications in near future. Recent improvement in the microfabrication technologies has led to the design of CMUTs that are more efficient than the piezoelectric transducer [21]. Though there have been many demonstrations of the ultrasonic transducers from early 1950's, Haller and Khuri-Yakub presented a landmark work in 1993 which was used in gas flow measurement and acoustic microscopy [22]. Since then, there has been extensive research in the design and fabrication of CMUTs [23-25]. There have also been a lot of system level advancements. Even though there are many advancements and innovation in fabrication of these CMUTs, still most of the medical imaging and the non destructive testing groups use the piezoelectric transducers instead of the CMUTs. There is still a long way to go before all the industries and hospitals use the capacitive ultrasonic transducers.

The cross sectional view of a CMUT is shown in Fig 2.1.

The main essential parts of CMUT are

1. Vacuum (cavity)
2. Membrane and
3. Electrodes.

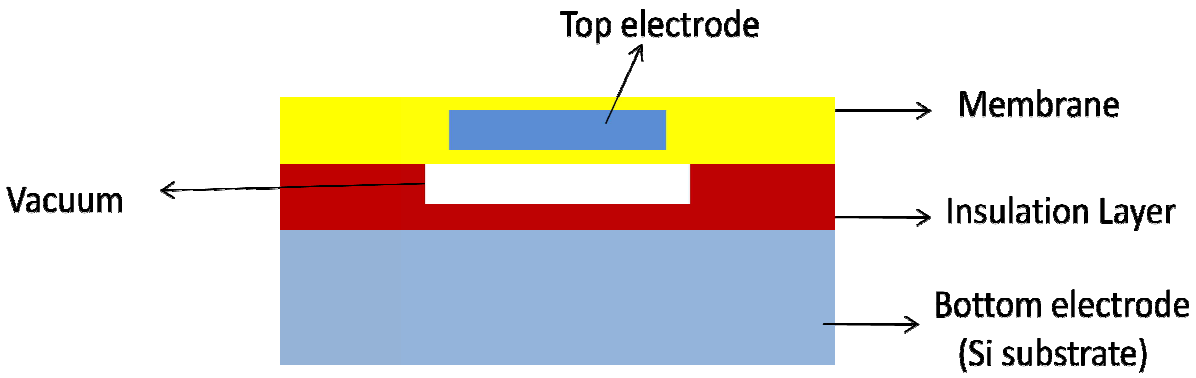

Figure 2.1: Cross section of a CMUT

1. The vacuum gap is very critical in determining the performance of a CMUT. It determines the dynamic range, sensitivity and coupling efficiency. The smaller the vacuum gap is, the higher the sensitivity and coupling efficiency are. Generally a good, high electrically resistive insulation material is needed to avoid destruction by short circuit.
2. In general, membranes are mostly silicon nitride, polysilicon or metals. If the membrane is an insulating material, there will be a thin layer of metal deposited in the middle of the membrane. The property of the material used for membrane such as density, stiffness, etc. is essential for the impedance matching between the membrane and the coupling medium. The coupling medium has generally low impedance. In order to achieve good impedance matching, the stiffness and density of membrane has to be selected carefully.
3. The bottom electrode in most of the case is silicon substrate since it is easy to micromachine with high accuracy. In general, the thickness of the silicon can be reduced

and it varies from 200-300 µm to reduce the acoustic loss. But in order to make the substrate foldable, it is essential to have the substrate less than 50 µm thick.

2.2 Principle of Operation

In a CMUT, the fundamental mechanism of the transducer is the vibration of a thin plate. It is very similar to the microphone operation [26]. It uses the deformation of a thin suspended membrane for transmitting and receiving ultrasonic waves. A CMUT performs chain of energy transformation in order to operate as a transducer. An AC signal is applied which causes the membrane to vibrate at the desired frequency due to electrostatic attraction force [27]. DC voltage is applied between the substrate and the metalized membrane, causing the membrane to be attracted towards the bulk silicon. Both AC and DC bias are required for smooth operation of a CMUT. Just like piezoelectric transducers, CMUTs also have reverse operation. If a CMUT receives ultrasound waves, the membrane deforms and thus the capacitance changes. Due to this capacitance change, there is current produced at the output.

In summary, there are two modes of operation of a transducer. They are

1. **Receiving mode** In this mode of operation, the acoustic energy is converted into mechanical energy and then into electric energy.
2. **Transmitting mode** In this mode of operation, electric energy is converted into mechanical energy and then into acoustic energy.

Figure 2.2 shows the operation of a transducer as a transmitter and a receiver.

The performance of the CMUT depends mainly on the applied DC bias. This DC bias should be close to collapse voltage of the CMUT for maximum transduction [28]. At the DC bias near the collapse voltage, very high electromechanical coupling can be achieved [29-30].

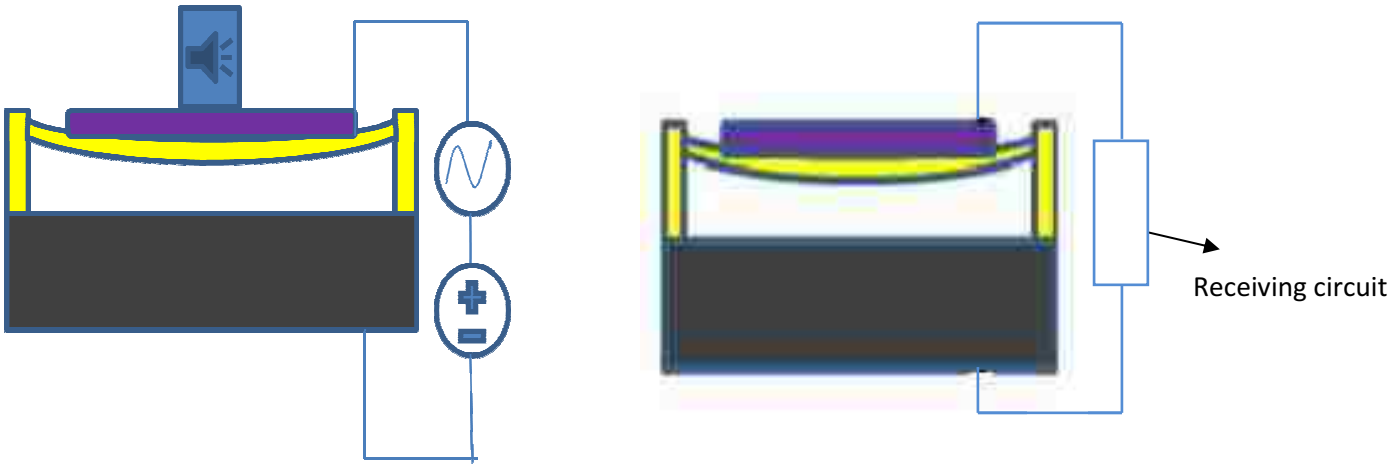

(a) (b)

Figure 2.2: Two modes of CMUT operation. (a) Transmitter mode (b) Receiver mode

2.3 Advantages of CMUTs over Piezoelectric Transducers

Traditionally piezoelectric transducers have been mainly used for ultrasound application which is mainly used for minimal invasive or non invasive imaging applications. Compared to the traditional piezoelectric transducers, capacitive micromechanical ultrasonic transducers are to replace piezoelectric transducers in the near future because of the number of advantages that they have. The main advantage of the CMUT over the piezoelectric transducer is that the impedance mismatch is very minimal i.e. the CMUTs have better impedance matching.

Ultrasound is reflected at the boundary where impedance varies. In a piezoelectric (bulk) transducer, the reflection of the ultrasound is more as there is large impedance mismatch between the lead zirconate titanate crystal and the surrounding medium.

Since the capacitive transducer has the membrane, the structure resists less motion and thus the ultrasound produced is more.

Also capacitive transducer can operate at wider temperature range compared to the bulk piezoelectric transducer [31]. Capacitive transducers can be fabricated using IC technology i.e. these can be integrated with the external signal processing and control circuits [32]. Another advantage a CMUT has is that it has less crosstalk between the nearing elements and also it can be operated at a wide range of frequency compared to the bulk piezoelectric transducers for which the operating frequency is fixed [33].

2.4 Design Parameters of an Ultrasonic Transducer

In designing an ultrasonic transducer, there are 5 main specifications which need to be taken care of [34].

They are

i. Probe dimension
ii. Resonant frequency of the suspended membrane
iii. Maximum membrane displacement
iv. Pull down voltage and
v. Maximum pressure of the acoustic wave.

Other parameters like the membrane thickness, the diameter of the membrane and the gap height are mainly determined by these specifications.

2.4.1 Probe Diameter

The main parameter above all is the probe or the catheter dimension. The probe can be flexible or rigid and is inserted into the human or animal body. The dimension of this probe generally varies with the application. In general, these probes are made up of polymers, mainly

silicone, this is because silicone is insensitive to the human body fluids. In general, the probe has to be small enough to slip into the sheath. The basic sheath size for an IVUS is approximately 8 Fr (2.7 mm) [35]. The IVUS probe is inserted into the sheath through the guide wire and then it is later directed into the human body.

2.4.2. Membrane Displacement and Sound Pressure

As mentioned in the previous chapter, the voltage applied between the membrane results in bending of the membrane and produces a pressure wave. Similarly, when a pressure wave is induced, the membrane deforms and results in the transducer being used as a receiver. The membrane displacements are also related to temperature changes. The membrane mean displacement (u_m) can be calculated by the volume displacement (u_v) which is related to the membrane deformation u. The equation below shows the mean membrane deformation. [36]

$$u_m = \frac{u_v}{S} = \frac{1}{S} \iint_S u \, dS$$

Where, S= surface area of the membrane.

The mean membrane displacement is also dependent on the sound pressure and its relation is as given.

$$u_m = \frac{P_m S}{K_r}$$

Where,

P_m= pressure

K_r= membrane stiffness

2.4.3. Resonant Frequency

As mentioned in the previous section, when an AC signal is applied to an ultrasonic transducer, the membrane vibrates and produces ultrasonic waves. The frequency at which the membrane vibrates vigorously and converts the electrical energy into mechanical energy efficiently is called as the resonant frequency. The vibration is maximum when the characteristic impedance is minimum. The resonant frequency mainly depends upon membrane radius, elasticity, thickness and loading.

The resonant frequency for a simple circular membrane which has its sides clamped is determined by the following equation. [37]

$$\omega = \frac{\lambda}{R^2}\sqrt{\frac{k}{\mu}}$$

Where,

R= radius of the membrane of uniform thickness.

λ= numerical value of circular membrane (a structure dependent value)

μ = ρt= mass of the plate per unit area

where,

ρ= plate material density

t= thickness of the plate

$k = \frac{Et^3}{12(1-\nu^2)}$ = bending stiffness

Where,

E= Young's modulus of the membrane

ν= Poisson's ratio

2.4.4 Pull-in Voltage

The DC bias voltage above which the membrane falls to the substrate is called as the collapse voltage or pull-in voltage. This phenomenon is also called as pull-in phenomenon. The value of the collapse voltage can be calculated by the FEM analysis [38]. After the membrane is collapsed, it is not released until the voltage is reduced back to snap-back voltage. The voltage at which the membrane goes back is called as the snap-back voltage. There has also been lot of research on operating the CMUT near the collapse voltage, near the snap-back voltage or in-between the collapse and the snap-back voltages [39-42].

Fig 2.3 shows the operation of a CMUT in collapse voltage i.e. the membrane has deformed and will not go back to its original position until the voltage is reduced to snap-back voltage or the voltages are completely removed.

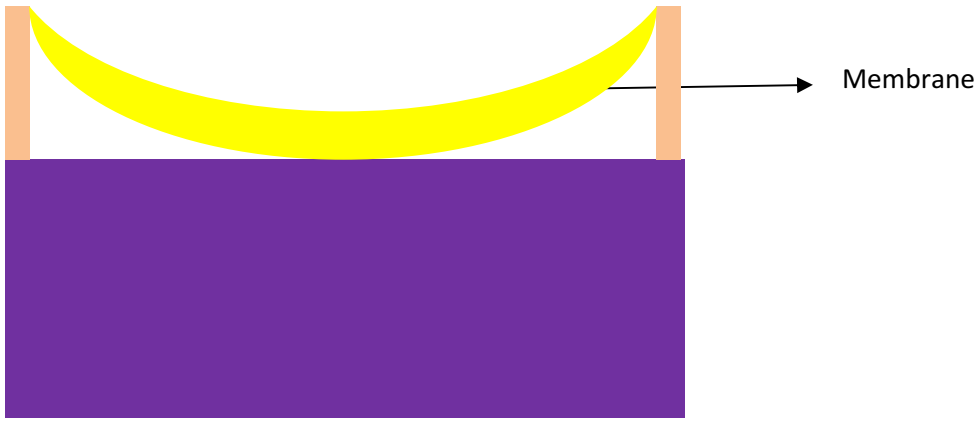

Figure2.3: Membrane pulled in.

The load deflection model for a circular membrane due to the uniform pressure (P) [44] is given as

$$P = \left[\frac{64k}{R^4}\right] w_0 + [\frac{128\ \alpha k}{t^2 R^4}] w_0^3$$

Where,

W_0= deflection

d_0= gap height

t= thickness of the membrane

α= Poisson ratio dependent empirical parameter

In order to effectively model the pull-in voltage, both electrostatic and restoring pressure should be taken into account.

The expressions for electrostatic and restoring pressure at pull-in are given by the following equations.

$$P_{electrostatic} = \in_0 V_{PI}^2 \left[\frac{5}{6d_0^2} + \frac{4}{3\pi R d_0} + \frac{1.918}{\pi R^2}\right]$$

$$P_{elastic} = \left[\frac{64k}{R^4}\right]\left(\frac{d_0}{3}\right) + \left[\frac{128\ \alpha k}{t^2 R^4}\right](\frac{d_0^3}{27})$$

By combining the above two equations, and solving for V_{PI}, we get

$$V_{PI} = \sqrt{\{\frac{\left[\frac{64k}{R^4}\right]\left(\frac{d_0}{3}\right) + \left[\frac{128\ \alpha k}{t^2 R^4}\right]\left(\frac{d_0^3}{27}\right)}{\in_0 \left[\frac{5}{6d_0^2} + \frac{4}{3\pi R d_0} + \frac{1.918}{\pi R^2}\right]}\}}$$

From the above equation, we can find the relation between the pull in voltage and the membrane dimension. The figure 2.4 shows the pull-in voltage.

Young's modulus: 210 X 10^9 N/m^2

Poisson's ratio: 0.27

Membrane radius= 200 µm

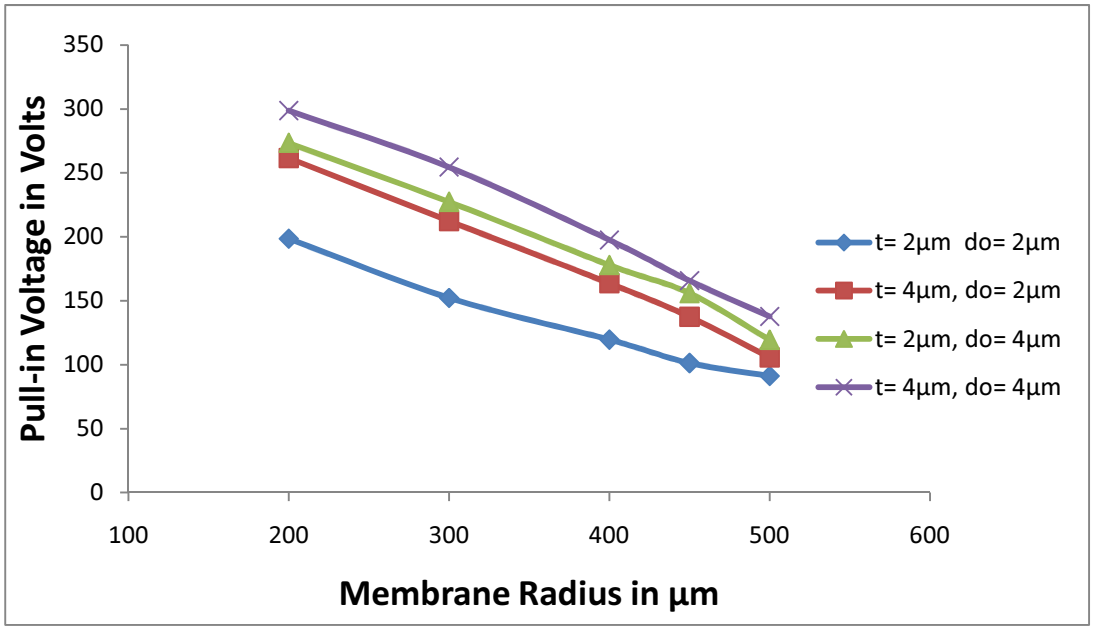

Figure 2.4: Membrane radius vs Pull-in voltage

2.5 ANSYS Simulation

In this chapter, the simulation for the calculation of resonant frequency is presented. The simulation was performed using finite element model (FEM) analysis. ANSYS was the software used for this analysis. The resonant frequency is of particular interest in designing CMUT because it indicates when the system will have maximum response. [45] Figure 2.4 shows the top membrane of a capacitive transducer which is cylindrical in shape. The material chosen for this simulation is silicon nitride. The properties of silicon nitride are as follows.

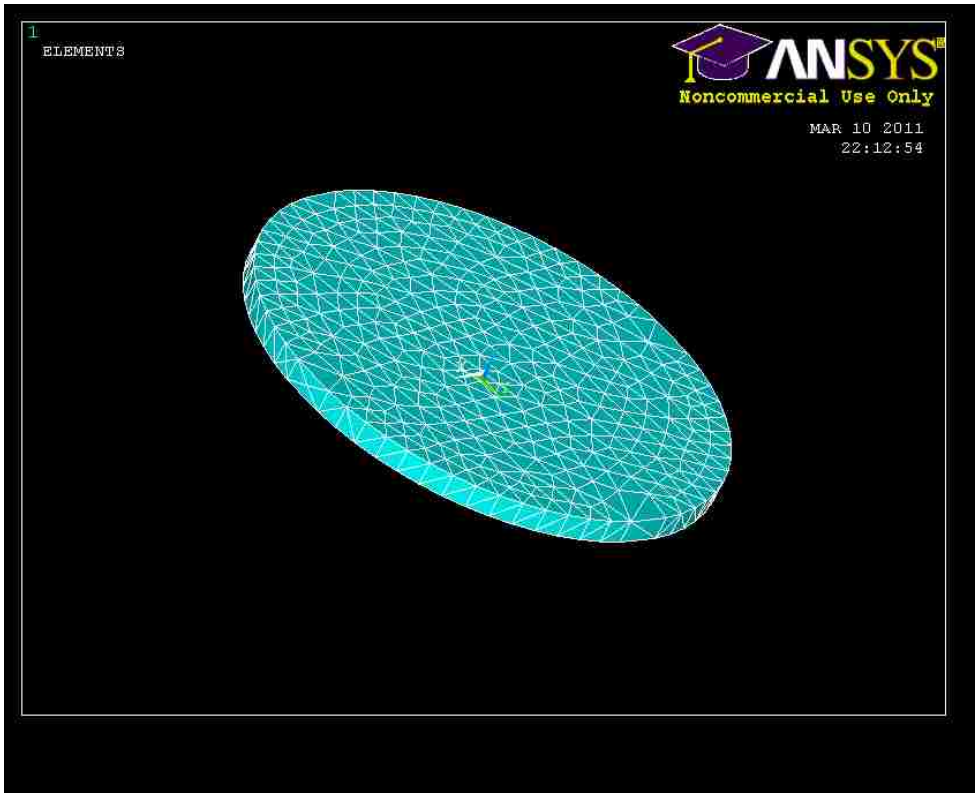

Figure 2.5: Meshed and modeled membrane for the study of resonant frequency with ANSYS

Young's modulus: 210 X 10^9 N/m^2

Poisson's ratio: 0.27

Numerical value: 0.86695

From the previous section, we can see that the resonant frequency of a material mainly depends on its thickness and radius. Therefore the graph showing the resonant frequency for different thickness and radius is shown in figure 2.6 and 2.7.

For a fixed radius of 100 µm, by varying the thickness the resonant frequency is shown in figure 2.5. Figure 2.6 shows the frequency for fixed thickness (20 µm) and varying the radius.

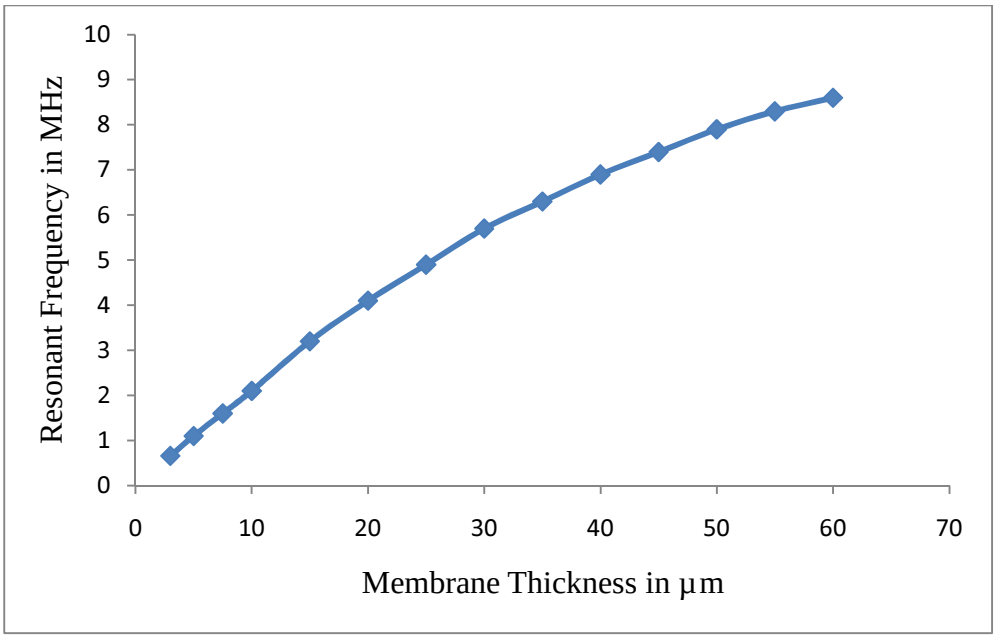

Figure 2.6: resonant frequency vs membrane thickness

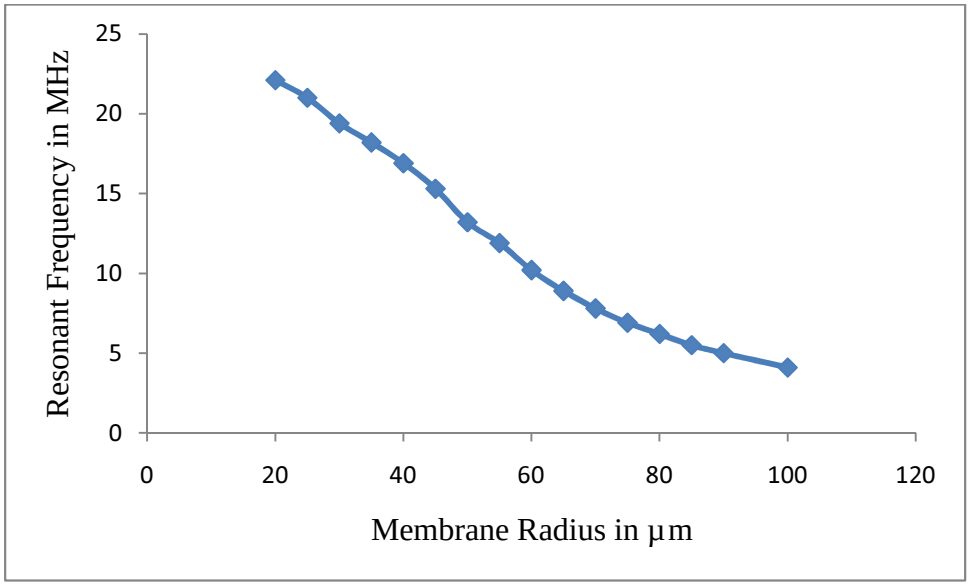

Figure 2.7: resonant frequency vs membrane radius

3. FABRICATION OF FOLDABLE SUBSTRATES

3.1 Preamble

In this chapter, the main principle and mechanism behind the folding of substrate is discussed. Next the design along with dimensions and materials are discussed in detail along with the process flow of the folding mechanism.

3.2 Folding Mechanism

As mentioned in Chapter 1, there are some applications where the flexible substrate is needed. In some areas where the substrate is needed to be conformed to an uneven surface, the flexible substrates are much needed. Also in some places where there is very little space for the transducers operation, flexible substrates are very useful. The flexible substrate will be possible by allowing radical configuration of micro-structure geometry. This can be realized by controlled out of plane rotation of substrate sections. The main principle behind rotation is the reflow of the material. This reflow is caused due to the surface tension. The very first realization of 3-D structure using the surface tension was by P.W.Green [46].

Previously the out-of-plane rotation was mainly by the mechanical hinges and manual assembly [47-49]. The power rotation can be done in many ways. They are [50]

1. Electromagnetic force
2. Polyimide shrinkage
3. Electrochemical swelling of polymers
4. Surface micro-machined vibro-motors and
5. Micro engines.

Here the polymer shrinkage is parallel and one time while the motors and engine are adjustable.

In this thesis we will be focusing on the polymer shrinkage in which the joints filled with polyimide is thermally rotated. The main advantage of using this process is that it is simple and easy to be combined with other process. The basic principle of polyimide shrinkage is shown in the figure 3.1. The polyimide shrinks when it is cured. The shrinkage is more at the top than the bottom which causes the polyimide to bend. The effective shrinkage can be found by the relation [51]. The effective shrinkage is an important parameter in polyimide selection.

$$\varepsilon = \frac{l_{uncured} - l_{cured}}{l_{uncured}}$$

Where,

$L_{uncured}$= Length of polyimide before curing.

L_{cured} = length of the polyimide after curing.

Bending angle =$\alpha = 2\{ 90^{o} - 54.74^{o} - \sin^{-1} (\cos (54.74) (1-\varepsilon) \}$

By connecting several V grooves in parallel, large bending angles can be obtained. Also the polyimide shrinkage is dependent on the curing temperatures and thus the angle can be somewhat controlled. The other way of having a flexible substrate is by using the polyimide as the substrate. The details about using the polyimide as the substrate will be give in the appendix A. Figure 3.2 shows the schematic diagram of a side looking transducer on a foldable substrate.

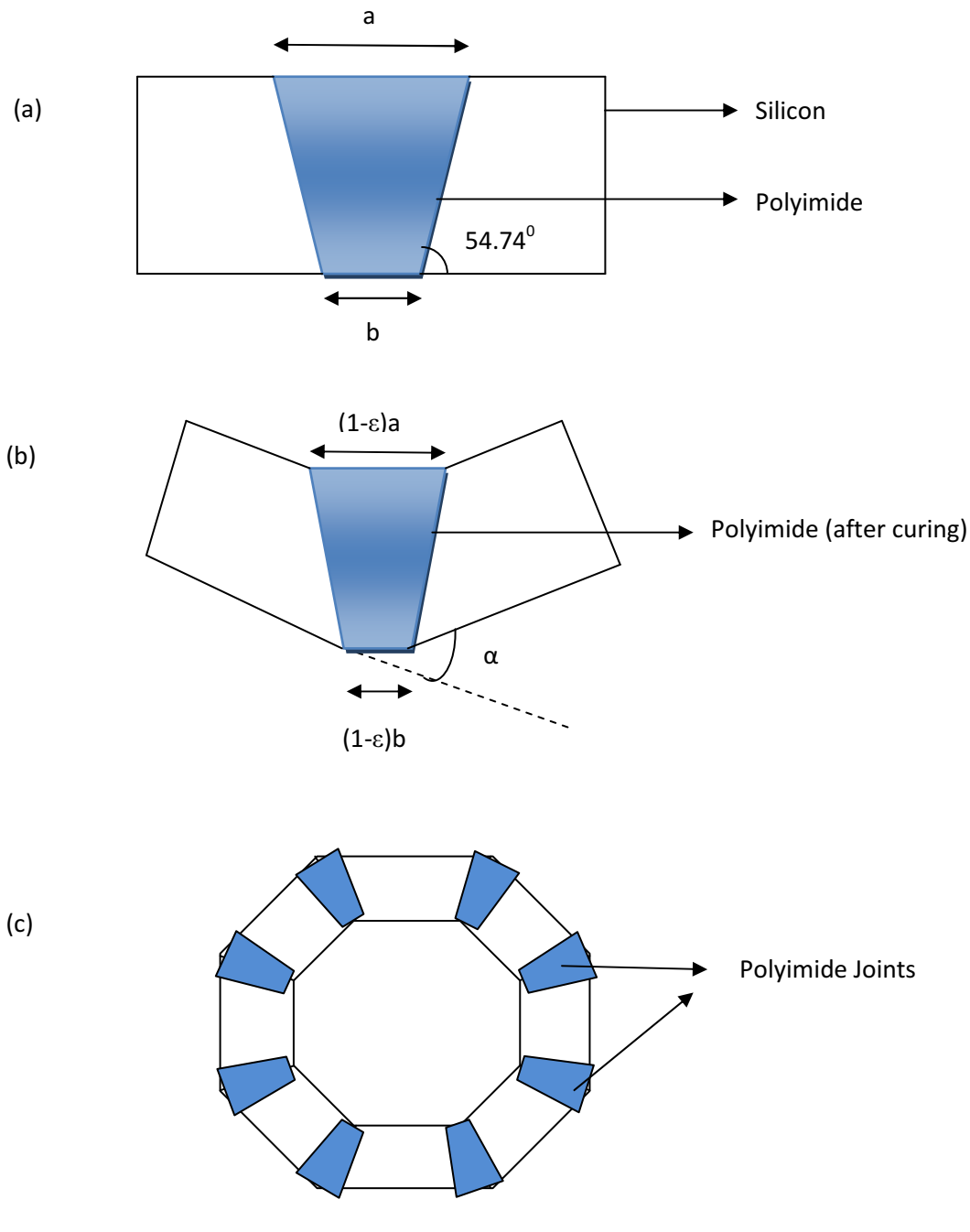

Figure 3.1: (a) Silicon substrate before curing of polyimide (b) Silicon substrate after curing of polyimide and (c) Simplified drawing of a folded substrate

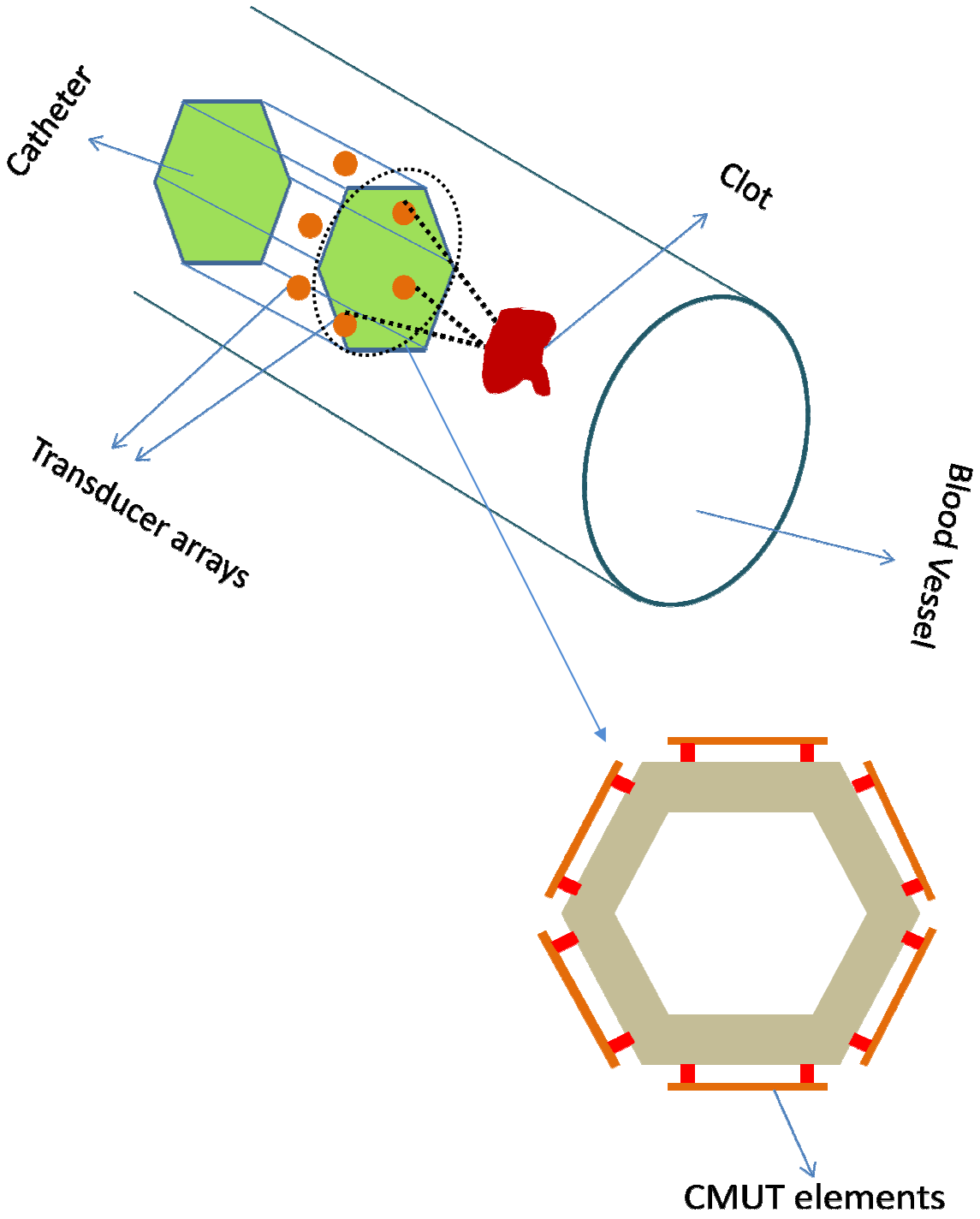

Figure 3.2: Schematic diagram of a side looking transducer array on a folded substrate.

3.3 Design

The design parameter of the foldable substrate mainly starts with the design of the mask for the lithography process. As mentioned before, the transducer is placed on the tip of the catheter which in turn is inserted into the human body. The diameter of the folded substrate should be almost 2 mm. Therefore the length of the sample should be approximately 6.2 mm. The main intention is to fabricate 64 elements which are about 90 µm wide for each element and 10 µm gap between each element. Now the next step is to find the suitable thickness of the substrate for opening V groove from back side KOH etching. The general thickness for the foldable substrate is around 30 µm to 50 µm. The SOI wafer was initially selected which has device layer of 30 µm and 50 µm.

The KOH forms an angle of 54.74^0 between the (100) and the (111) plane. By using the basic trigonometric formula the mask opening can be calculated. The calculated mask openings and the polyimide pattern dimensions are as follows.

1. For 30 µm

    Opening for KOH= 47.5 µm

    Gap between openings= 54 µm

    PI pattern opening= 74 um

2. For 50 µm

    Opening for KOH= 64.5 um

    Gap between opening= 36.5 µm

PI patterning= 56.5 µm

Figure 3.3 show the mask opening with the dimensions illustrated and figure 3.4 shows the mask layout for 50 µm thick substrate for both KOH and polyimide patterning.

The next step was to select a suitable polyimide for folding the substrate into a circular shape. The shrinkage property of the polyimide plays a huge role here. The polyimide was selected such that it has good shrinkage property and also considerably good mechanical strength. The mechanical properties of the polyimide are as given below.

Tensile strength: 260 MPa

Stress: 18 Mpa

Thermal expansion coefficient (1 µm thick film): 13 ppm

Thermal expansion coefficient (10 µm thick film): 20 ppm

Total shrinkage (liquid - cured) = 83%

Total shrinkage (soft bake to cured) = 12%

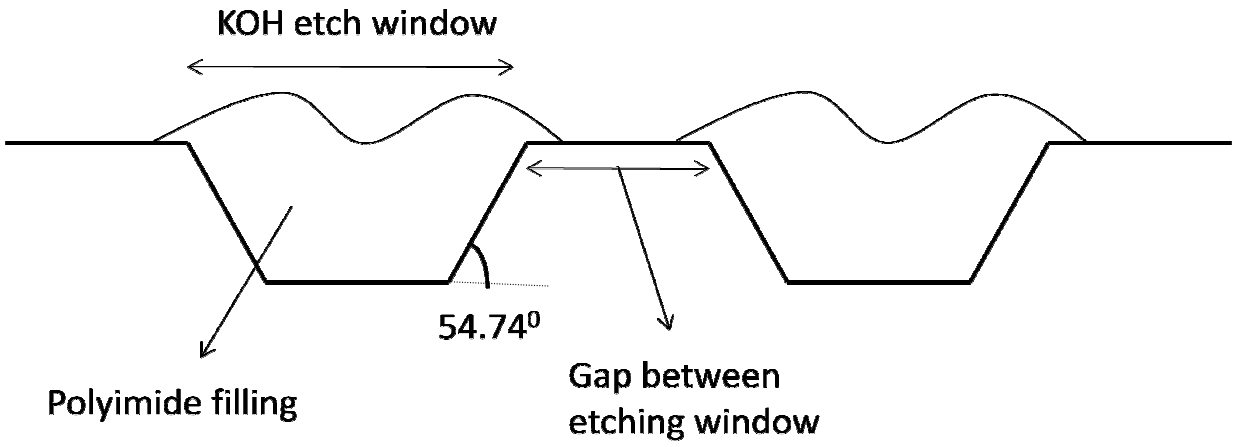

Figure 3.3: Mask opening dimensions for KOH etch

3.4 SOI Substrate

The main objective of this thesis is to develop a foldable substrate for IVUS transducers. Although there have been many theories about the folding mechanism to form a 3D structure, the foldable silicon substrate is new of its kind. In order to make the substrate foldable, the silicon wafer used should be as thin as possible. The initial experiment for making the substrate foldable was conducted using silicon on insulator (SOI) wafer.

An SOI wafer consists of a base/handle silicon layer of 550 µm thickness, buried oxide of 1.5µm thickness and device silicon layer of 50 µm thicknesses. First the handle silicon layer should be removed. The handle layer can be removed by wet etching, i.e. by using potassium hydroxide (KOH) solution. There are quite a few challenges faced in KOH etching where a thick 550 µm layer has to be etched through. In order to protect the front side of the SOI wafer, a mechanical glass slide and silicone was used. The silicone used in this application is poly-di-methyl siloxane also known as PDMS. PDMS was sealed around the silicon such that the KOH does not penetrate to the front side.

Figure 3.4 shows the cross section of PDMS sealing an SOI wafer. Although the KOH etching using this method was successful, there were issues in subsequent steps. Even though most of the handle silicon was removed by KOH, there still remained the walls made by the KOH etching (550 µm thick) which became hindrance in the subsequent contact lithography, i.e. it resulted in poor resolution. In order to avoid these issues, ultrathin wafer of 50 µm thickness was used as the substrate. The basic design details and the fabrication flow of a foldable substrate using a ultrathin wafer are explained in section 3.5.

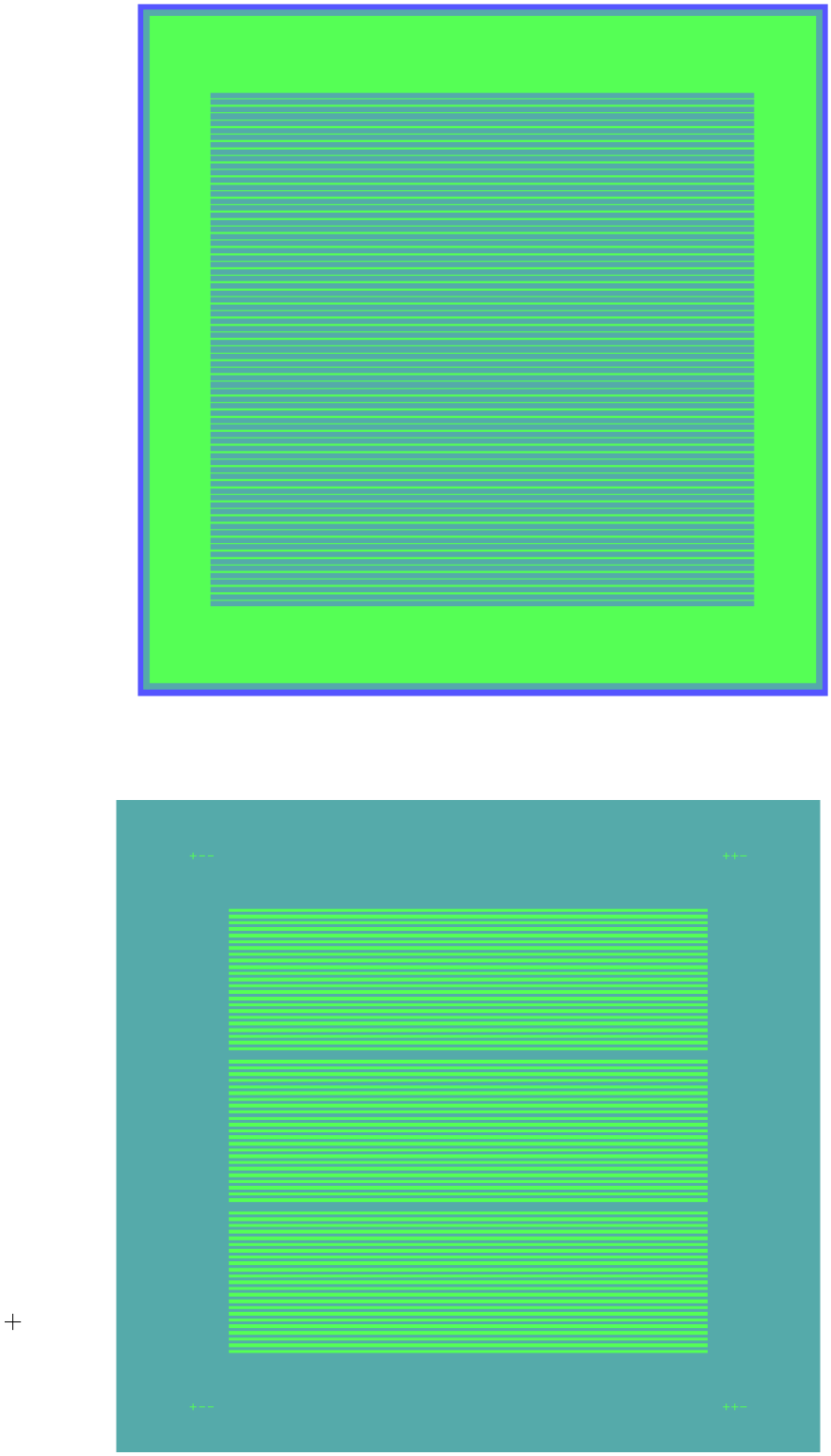

Figure 3.4: Mask layout for 50 µm thick substrate. **Top:** KOH mask. **Bottom:** Polyimide mask

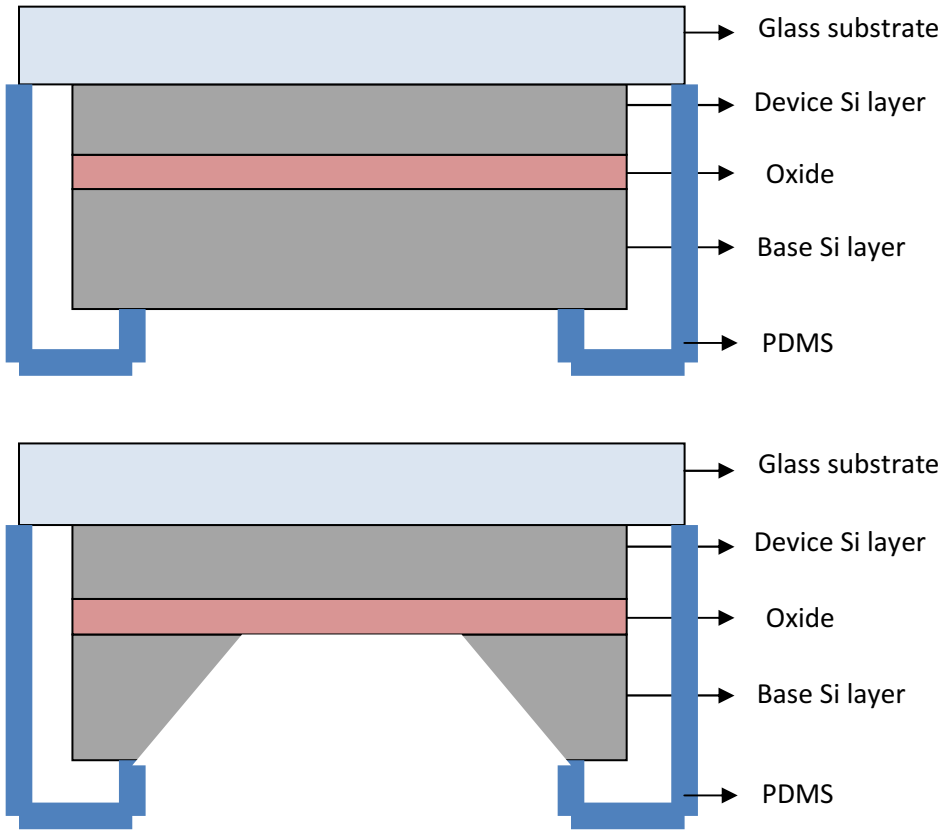

Figure 3.5: PDMS seal for KOH etching of an SOI wafer

3.5 Process Flow

The ultrathin silicon wafer which was bought from the University Wafers is used as the substrate. The basic fabrication process is shown step by step in figure 3.6.

Figure 3.6 Fabrication process flow of the foldable substrate

(Figure 3.6 continued)

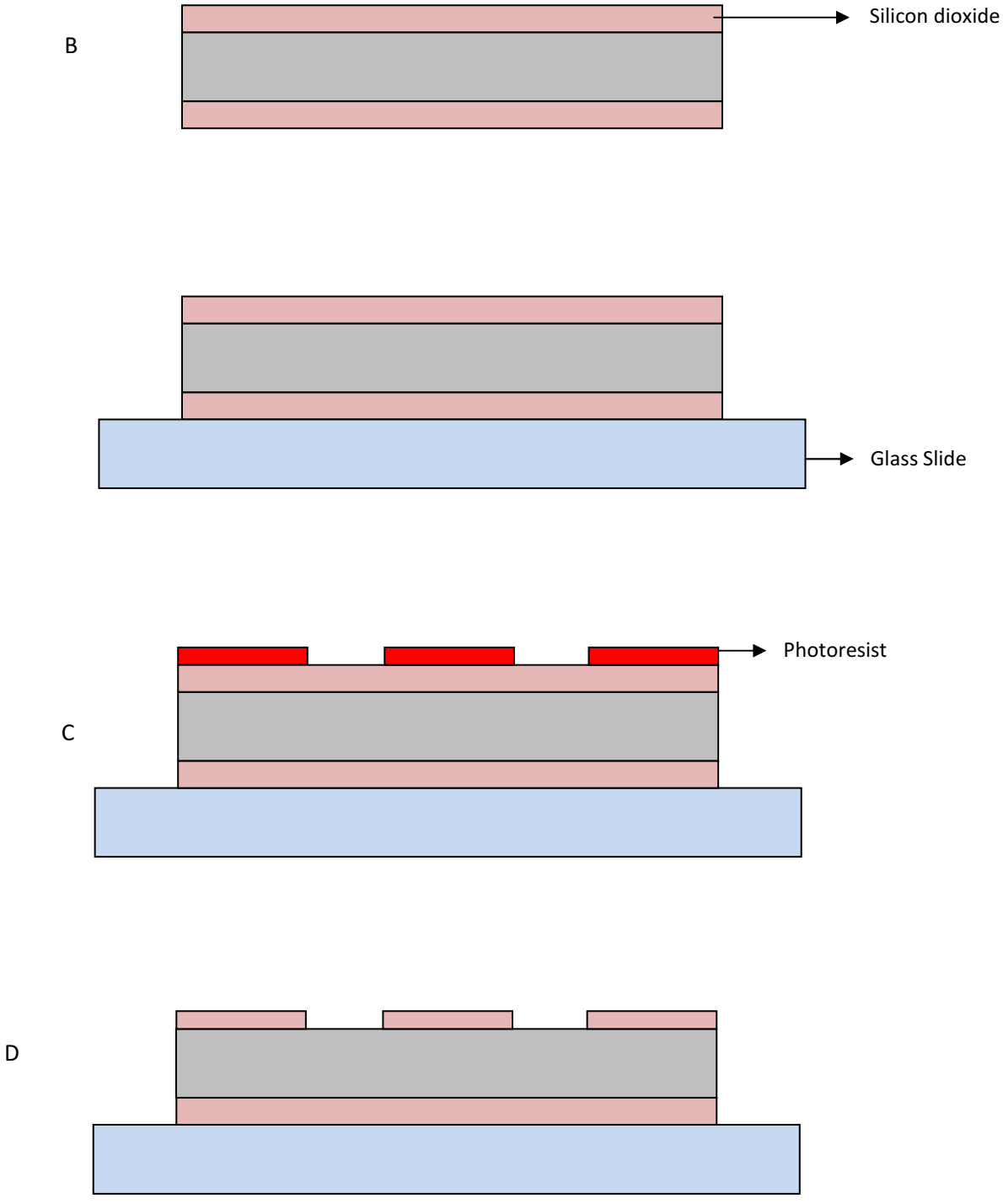

(Figure 3.6 continued)

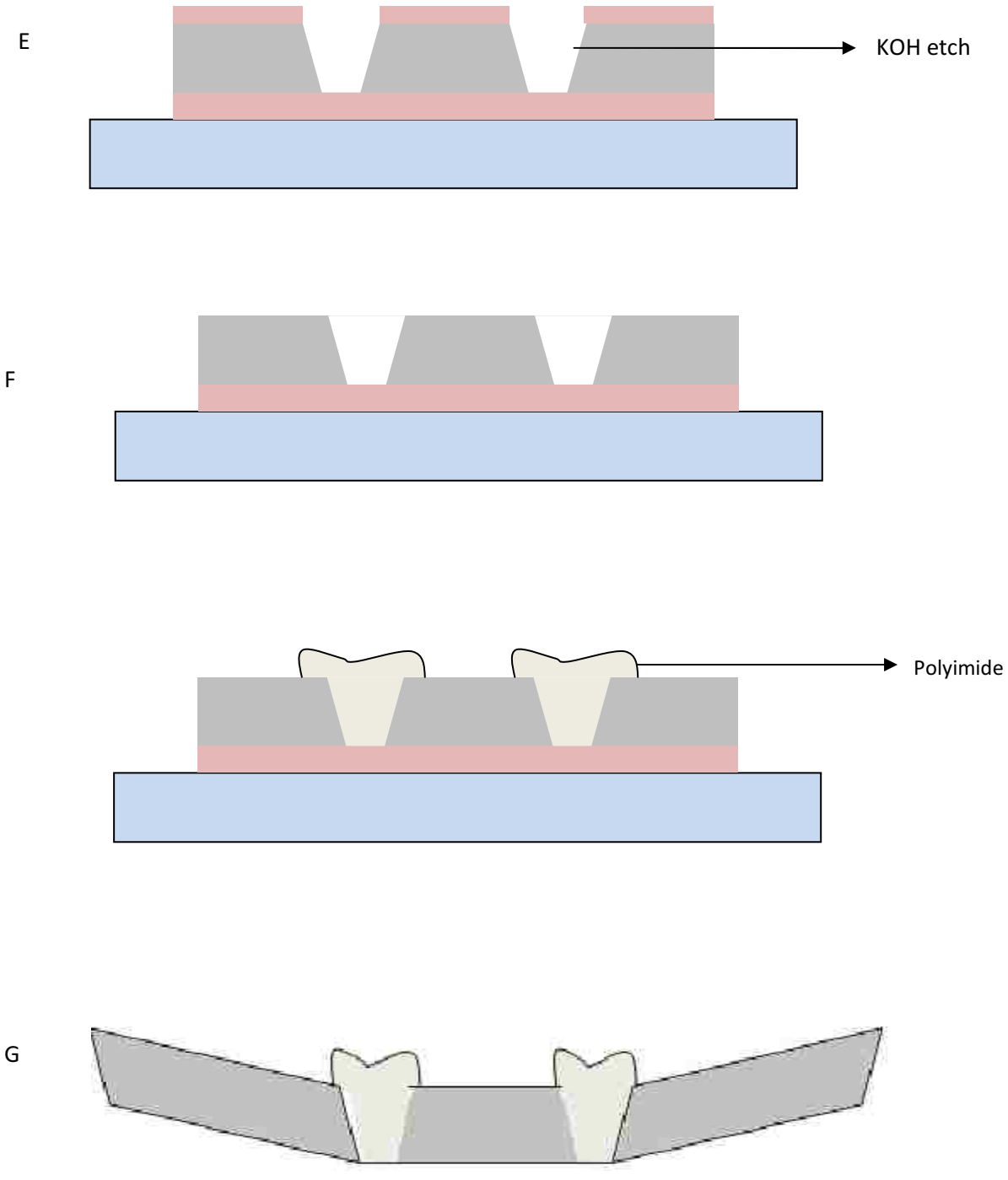

A. Sample Preparation

First the ultrathin wafers (diameter: 4", thickness: 50 µm) is cleaved approximately into 0.75"x0.75". After cleaving, the samples are cleaned in Piranha (mixture of concentrated sulphuric acid and hydrogen peroxide in the ratio 2:1) solution in order to get rid of organic impurities. Then they are dipped into acetone, methanol and DI water for further cleaning. Once the sample is cleaned, the next step is to oxidize the sample for an etch mask in subsequent wet etching process.

B. Thermal Oxidation

The cleaned samples are then loaded into the oxidation chamber. Axcess Integrator Loader of MRL Industries is the oxidation furnace used. The oxidation parameters are as follows.

1. Temperature =1000^{o} C
2. Time =24 Hrs
3. Oxygen flow rate=2.5 sccm

By these parameters, 400 nm of silicon dioxide was grown. Even though silicon nitride is much more reliable etch mask against KOH compared to silicon dioxide [52], silicon dioxide was still used considering the ease of fabrication and also relatively short duration required for KOH etching.

C. Photolithography

Once the samples are oxidized they are then attached to a mechanical substrates, i.e. microscope slides by using Protek B3. Protek B3 was chosen because it can withstand high temperature and also can be easily removed by dipping it in acetone. The Protek B3 applied on

the microscope slide is then allowed to set at room temperature for 4 hours. Once the sample is attached to the microscope slide it is then patterned. The photolithography process consists of the following steps

1. Spin coating of AZ9260 photo resist (recipe given in Appendix-B).
2. Soft baking for 20 min at 95^{o}C in furnace.
3. Allowing rehydration time for 20 min. This helps in avoiding bubbles during exposure.
4. Exposure using Karl-Suss with an UV intensity of 9.8 mW/cm^2 for 1.7 min.
5. Development in 3:1 diluted AZ400K developer for approximately 4 to 5 min.
6. RIE oxygen plasma for 10 min in order to remove photoresist residue.

By the above procedure etching patterns are formed and the Fig 3.7 shows the microscope picture of the patterns.

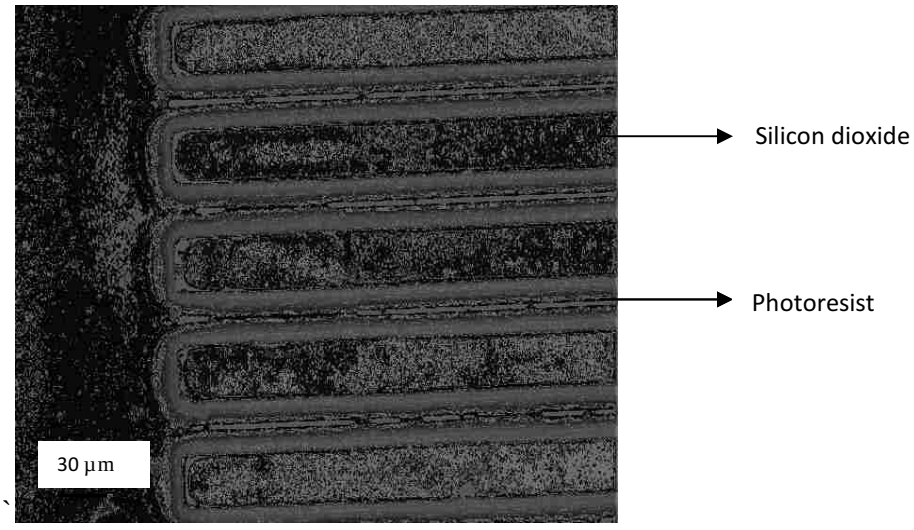

Figure 3.7: After first lithography (top view)

D. Dry Etching of Silicon Dioxide:

The next step in order to do wet etching of silicon to form V groove is to expose silicon underneath the silicon dioxide layers. Therefore, the SiO_2 layer should first be removed. This is done through dry reactive ion etching (RIE). The equipment used was plasma system 100 from Oxford Instruments at Center for Advanced Microstructures and Devices (CAMD).

The RIE parameters are as described below.

1. Atmosphere: CF_4 gas plasma
2. Flow rate : 20 sccm
3. Time : 8 minutes (etch rate: approximately 50 nm/min)
4. Power: 200 watts.

Figure 3.8 shows the patterns after dry etching.

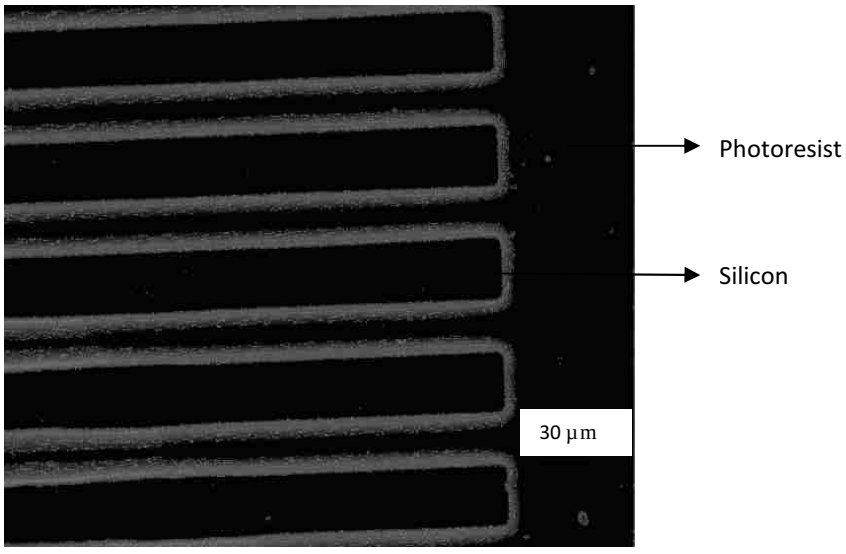

Figure 3.8: Silicon exposed after dry etching of silicon dioxide

E. Protection of Front Side and Wet KOH Etching

After RIE, samples are now ready for wet KOH etching for the V grooves. In order to protect the front side, it is sealed with PDMS and allowed to cure at 80^{o}C for 2 hours. After curing, the PDMS is allowed to set at room temperature for 15 hours in order to attain its full chemical properties. Now the photoresist at the back is removed by acetone and then it is dipped in the KOH bath. The KOH bath consists of

1. 70 g of KOH pellets.
2. 190 ml of DI water.
3. 40 ml of isopropyl alcohol.

Isopropyl alcohol is used in order for smooth etching of silicon. The KOH etching is done at 70^{o} C for 110 min with a etch rate of 0.4 µm/min. Figure 3.9 shows the V-groove formed after KOH etching

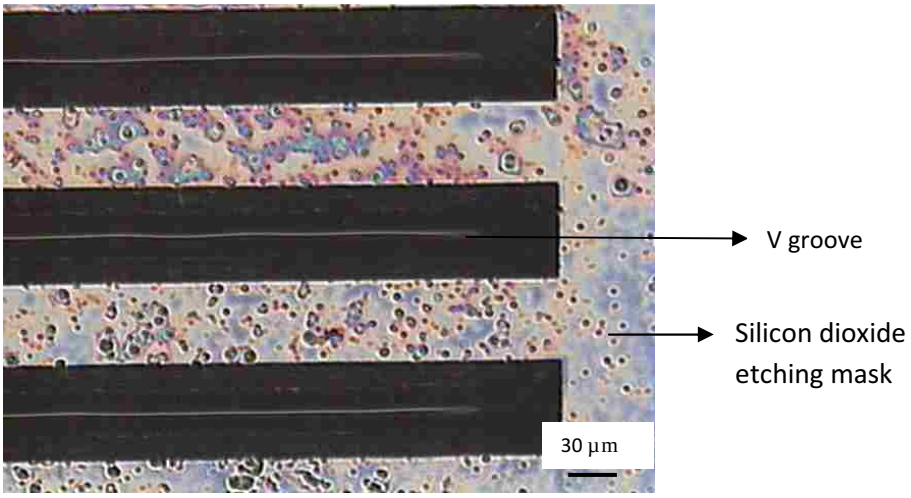

Figure 3.9: V grooves formed by the KOH etching

F. Polyimide Patterning

After the V grooves are formed the remaining oxide from the backside is removed in HF. The sample is now ready for polyimide patterning. The steps involved in polyimide patterning are as follows.

1. Spin coat VM 651 an adhesion promoter.
2. Soft bake at 120^{o}C for 1 min.
3. Spin coat PI 5878G polyimide (recipe in Appendix-B).
4. Soft back at 135^{o}C for 5mins.
5. Spin coat AZ 9260 Photoresist.
6. Polyimide mask alignment with V groove of the silicon using OAI Hybalign Series 200.
7. Develop in AZ 400K developer for 4-5 min.
8. RIE etching in oxygen plasma for 75 min to remove the polyimide.

Figure 3.10 shows the polyimide patterned substrate treated with oxygen plasma

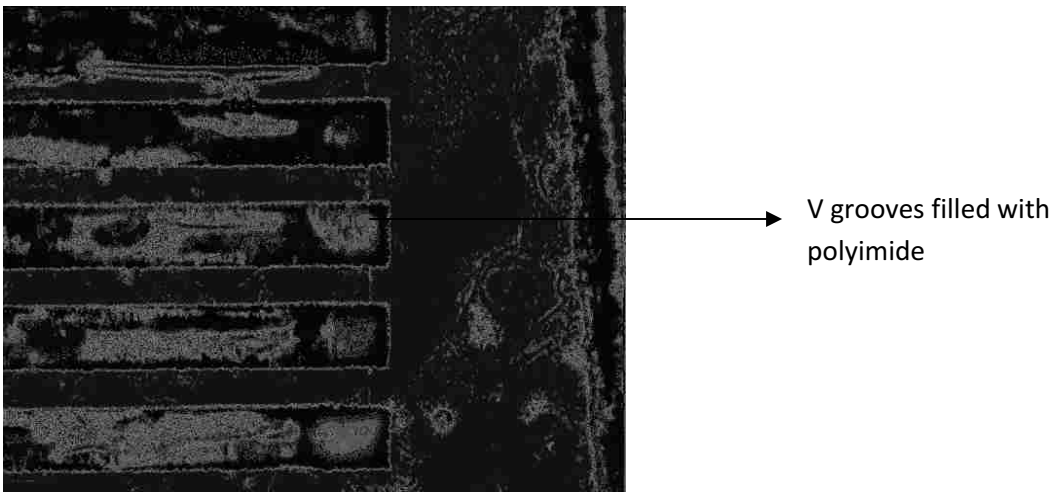

Figure 3.10: After polyimide patterning

G. Curing and Folding of Substrate

Once the polyimide is patterned, final step is to dice the sample and cure the polyimide at either air or nitrogen ambient at 350^{o}C for 1 hour. The curing conditions are as follows.

1. Ramp temperature to 200^{o} C at 4^{o}C/min.
2. Hold at 200^{o}C for 30 min.
3. Ramp from 200^{o}C to 350^{o}C at 2-3^{o}C/min.
4. Cure at 350^{o}C for 1 hour.

The final output would be a folded silicon substrate.

3.6 Result and Future Work

The final result of the current work is the folded substrate for capacitive transducers for IVUS and EUS applications. The result obtained is shown in the figure 3.11. The sample was just partly folded because of the breakage of sample. The issue arrived when the sample was tried to detach from the mechanical glass substrate. The initial idea was to detach the sample through acetone from protek B3. The polyimide arrived at the interface of the acetone and protek B3 thus making it tough to remove from the glass.

The future work in this work would be to fold the substrate to form a circle by carefully detaching it from glass. Also the next step would be to design and fabricate ultrasonic transducers such that they are on the foldable substrate.

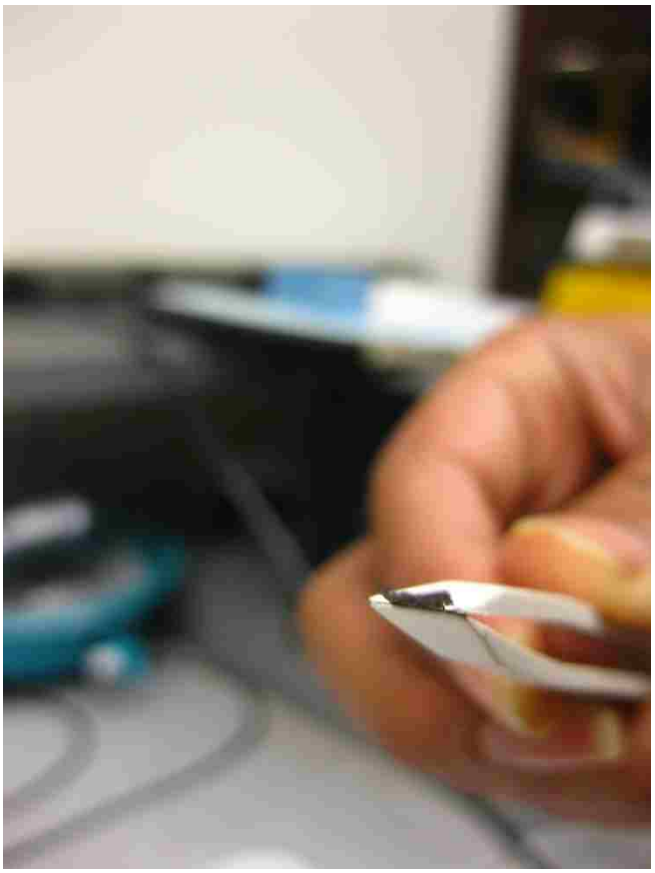

Figure 3.11: Folded substrate

4. CONCLUSION

The CMUT and its advantages compared to the piezoelectric transducers were discussed. The ANSYS simulation was performed in order to find the resonant frequencies of the membrane of CMUTs at different conditions. The focus was mainly on a foldable substrate and the fabrication of the same. The foldable substrate was achieved partially and several issues related to the flexible substrates were discussed.

BIBLIOGRAPHY

1. Medical Ultrasonography. (n.d.). Retrieved April 6, 2011, from Medical Supplies & Equipment Company: http://diagnostic-supplies.medical-supplies-equipment company.com/PPF/page_ID/171/article.asp

2. Ultrasonography. (n.d.). Retrieved April 19, 2011, from SonographyTraining.net: http://www.sonographytraining.net/Ultrasonography.html

3. Sokolvo, S. Y. "On the problem of the propagation of ultrasonic oscillations in various bodies." Elek. Nachr. Tech. 6:454-460, 1929.

4. Dussik, K. T. "On the possibility of using ultrasound waves as a diagnostic aid." Neurol. Psychiat. 174:153-168. 1942.

5. Fenster, A., Downey, D. B., & Cardinal, N. H. (2001). Three-dimensional ultrasound imaging. Physics in Medicine and Biology , R67-R99.

6. Ultrasonography. (n.d.). Retrieved April 20, 2011, from www.baby2see.com: http://www.baby2see.com/medical/ultrasonography.html

7. Omer Oralkan, " Acoustical Imaging Using Capacitive Micromachined Ultrasonic Transducer Arrays: Devices, Circuits, and Systems", Ph.D dissertation, Stanford University, March 2004.

8. Xiaoyang Cheng, "Minimally invasive capacitive micromachined ultrasonic transducer arrays for biomedical applications", Ph.D dissertation, University of New Mexico, August 2008

9. Khandpur, R. (2009). Handbook of Biomedical Instrumentation. New Delhi: Tata McGraw Hill.

10. Daniel Gologorsky, Amy C Schefler, Fiona J Ehlies, Paul A Raskauskas, Yolanda Pina, Basil K Williams Jr, Timothy G Murray, "Clinical imaging and high-resolution ultrasonography in melanocytoma management.", Journal of clinical ophthalmology, July 2010

11. Emmanuel Chérin, Jeremy Brown, Svein-Erik Måsøy, Hamid Shariff, Raffi Karshafian, Ross Williams, Peter N. Burns and F. Stuart Foster, "Radial Modulation Imaging of Microbubble Contrast Agents at High Frequency." Ultrasound in medicine and biology, June 2008

12. Acoustic Impedance. (n.d.). Retrieved April 24, 2011, from www.ndt-ed.org.: http://www.ndtd.org/EducationResources/CommunityCollege/Ultrasonics/Physics/acousticimpedance.htm

13. Endoscopic Ultrasound (EUS). (n.d.). Retrieved April 26, 2011, from MedicineNet.com: http://www.medicinenet.com/endoscopic_ultrasound/article.htm

14. IVUS Overview. (n.d.). Retrieved April 26, 2011, from Angioplasty.Org: http://www.ptca.org/ivus/ivus.html

15. Douglas M. Cavaye, Rodney A. White. Intravascular Ultrasound Imaging, Raven Press.1993.

16. Omer Oralkan, Sean T. Hansen, Baris Bayram, Goksen G Yarahoglu, A. Sanli Ergun, and Butrus T. Khuri-Yakub, "CMUT Ring Arrays for Forwad-Looking Intravascular Imaging," Proceedings of the 2004 IEEE Ultrasonics Symposium, pp.403-406.

17. Joshua G. Knight and F. Levent Degertekin, "Capacitive Micromachined Ultrasonic Transducers for Forward Looking Intravascular Imaging Arrays," Proceedings of the 2002 IEEE Ultrasonics Symposium, pp. 1079-1082.

18. Y. Wang, D. N. Stephens, and M. O'Donnell, "A Forward-Viewing Ring-Annular Array for Intravascular Imaging," Proceedings of the 2001 IEEE Ultrasonics Symposium, pp. 1573-1576.

19. A.Ballato, "Piezoelectricity: old effect, new thrusts," IEEE Trans. Ultrasonic, Ferroelectric., Freq. Cont., Vol. UFFC-42, pp.916~926, Sep. 1995.

20. S.Fujishima, "The history of ceramic filters," IEEE Trans. Ultrason., Ferro-elect.,Freq. Cont., vol. UFFC-47, pp 1~7, Jan 2000.

21. Khuri-Yakub. (n.d.). Brief History of CMUTS. Retrieved May 1, 2011, from Semizone Information service: http://www.kyg.stanford.edu/khuriyakub/opencms/en/research/cmuts/History/index.html

22. M. I. Haller and B. T. Khuri-Yakub, "A surface micromachined electrostatic ultrasonic air transducer," in Proc. IEEE Ultrason. Symp., 1994, pp. 1241-1244.

23. X. C. Jin, I.Ladabaum, and B. I. Khuri-Yakub, "The microfabrication of capacitive ultrasonic transducers," J. Microelectromech. Syst., vol. 7, no.3, pp 295~302, Sept. 1998.

24. X. C. Jin, I. Ladahaum, F. L.Degertekin, S. Calmes and B. T. Khuri-Yakub, "Fabrication and characterization of surface micromachined capacitive ultrasonic immersion transducers," IEEE/ASME J. Microelectromech. Syst., vol.8, pp. 100-114, Mar. 1999.

25. B. T. Khuri-Yakub, C. -H Cheng, F. L. Degertekin., S. Ergun, S. Hansen, X. C. Jin, and O. Oralkan "Silicon micromachined ultrasonic Transducers, "Jpn. J.Appl. Phys., vol. 39, pp 2883~2887, May 2000.

26. Arif S. Ergun; Goksen G. Yaralioglu; and Butrus T. Khuri-Yakub, "Capacitive Micromachined Ultrasonic Transducers: Theory and Technology." Journal of aerospace engineering, pp 76-84, April 2003

27. Joshua Knight, Jeff McLean, and F. Levent Degertekin, Member, IEEE, ". Low Temperature Fabrication of Immersion Capacitive Micromachined Ultrasonic Transducers on Silicon and Dielectric Substrate.", IEEE transactions of ultrasound, pp 1324-1333, Occtober 2004.

28. I. Ladabaum, X. Jin, H. T. Soh, A. Atalar, and B. T. Khuri-Yakub, "Surface micromachined capacitive ultrasonic transducers", IEEE Trans. on UFFC, Vol. 45, No. 3, pp. 678-690, May 1998.

29. Yaralioglu GG, Ergun AS, Bayram B, Haggstrom E, Khuri-Yakub BT. Calculation and measurement of electromechanical coupling coefficient of capacitive micromachined ultrasonic transducers. IEEE Trans. Ultrason, Ferroelect., Freq. Contr 2003;vol. 50(No 4)

30. Olcum S, Senlik MN, Atalar A. Optimization of gain-bandwidth product of capacitive micromachined ultrasonic transducers. IEEE Trans. Ultrason, Ferroelect., Freq. Contr 2005;vol. 52(No 12)

31. P. Eccardt, K. Niederer, T. Scheiter, and C. Hierold, "Micromachined transducers in CMOS technology," in Proc.Ultrason. Symp., p.959-962, 1996

32. X.C. Jin, I. Ladabaum, L. Degertekin, S. Calmes, and B.T. Khuri- Yakub, "Fabrication and characterization of surface micromachined capacitive ultrasonic transducers," IEEE J. Microelectromechanical Systems., vol. 8(1), p.100-114, Mar. 1999.

33. Serena H. Wong, Mario Kupnik, Kim Butts-Pauly, and Butrus T. Khuri-Yakub, "Advantages of Capacitive Micromachined Ultrasonics Transducers (CMUTs) for High Intensity Focused Ultrasound (HIFU)" IEEE ultrasonic symposium, 2007

34. Chen, J., Cheng, X., Chen, C.-C., & Li, P.-C. (2008). 41. A Capacitive Micromachined Ultrasonic Transducer array for minimally invasive medical diagnosis. . Journal of Microelectromechanical Systems , 599-610.

35. Marc Passman MD, "IVUS Guided IVC Filter Placement: Single vs. Dual Puncture Access and Other Technical Tricks."

36. O.Brand, H.Baltes and U. Baldenweg, "Ultrasound transducer using membrane resonators realized with bipolar IC technology", proceedings in IEEE MEMS'94. 38-43, Oiso, Japan, 1994.

37. T.B. Avallone and E.A.Avallone, Mark's standard handbook for mechanical engineers, 10th edtion. New York: McGraw Hill 1996

38. A. Nikoozadeh, B. Bayram, G. G. Yaralioglu, and B. T. KhuriYakub, "Analytical calculation of collapse voltage of cMUT membrane," in Proc. IEEE Ultrason. Symp., 2004, pp. 256–259

39. B. Bayram, E. Hæggstr¨om, G. G. Yaralioglu, and B. T. KhuriYakub, “A new regime for operating capacitive micromachined ultrasonic transducers,” IEEE Trans. Ultrason., Ferroelect.,Freq. Contr., vol. 50, pp. 1184–1190, Sep. 2003.

40. Y. Huang, E. Hæggstr¨om, B. Bayram, X. Zhuang, A. S. Ergun, C. H. Cheng, and B. T. Khuri-Yakub, “Collapsed regime operation of capacitive micromachined ultrasonic transducers based on wafer-bonding technique,” in Proc. IEEE Ultrason. Symp., 2003, pp. 1161–1164.

41. B. Bayram, ¨O. Oralkan, A. S. Ergun, E. Hæggstr¨om, G. G. Yaralioglu, and B. T. Khuri-Yakub, “Capacitive micromachined ultrasonic transducer design for high power transmission,” IEEE Trans. Ultrason., Ferroelect., Freq. Contr., vol. 52, no. 2, pp. 326–339, Feb. 2005.

42. B. Bayram, E. Hæggstr¨om, A. S. Ergun, G. G. Yaralioglu, and B. T. Khuri-Yakub, “Dynamic analysis of CMUTs in different regimes of operation,” in Proc. IEEE Ultrason. Symp., 2003, pp. 481–484.

43. Arif S. Ergun; Goksen G. Yaralioglu; and Butrus T. Khuri-Yakub, “Capacitive Micromachined Ultrasonic Transducers: Theory and Technology.” Journal of aerospace engineering, pp 76-84, April 2003

44. S. Timoshenko and S. Woinowsky-Krieger, *Theory of Plates and Shells*, McGraw-Hill Book Company New York, 1959, pp. 397-428

45. S A Anbalagan, G Uma and M Umapathy, “Modeling and simulation of Capacitive Micro machined Ultrasonic Transducer (CMUT)”, IEEE

46. P. W. Green, R. R. **A.** Syms, and E. M. Yeatman, “Demonstration of Three-Dimensional Microstructure Self- Assembly”, JOURNAL OF MICROELECTROMECHANICAL SYSTEMS, VOL. 4, NO. 4, DECEMBER 1995

47. K. Suzuki, I. Shimoyama, H. Miura, and Y. Ezura, “Creation of an insect-based microrobot with an external skeleton and elastic joints,” in *Proc. Micro Electro Mechanical Systems ’92*, Travemunde, Germany, Feb. 4–7, 1992, pp. 190–195.

48. K. Suzuki, I. Shimoyama, and H. Miura, “Insect model based microrobot with elastic hinges” J. Microelectromech. Syst., vol. 3, pp. 4–9, 1994.

49. M. G. Allen, M. Scheidl, and R. L. Smith, “Design and fabrication of movable silicon plates suspended by flexible supports,” in Proc. IEEE Microelectromechanical Syst. Workshop, Feb. 1989, pp. 76–81.

50. Surface Tension Powered Self-Assembly of 3-D Micro-Optomechanical Structures, Richard R. A. Syms, JOURNAL OF MICROELECTROMECHANICAL SYSTEMS, VOL. 8, NO. 4, DECEMBER 1999

51. Thorbjorn Ebefors, Edvard Kalvesten and Goran Stemme , “New small radius joints based on thermal shrinkage of polyimide in V-grooves for robust self-assembly 3D microstructures,” , J. Micromech. Microeng. 8 (1998) 188–194.

52. M. Bachman, “Anisotropic Silicon Etch Using KOH”, UCI Integrated Nanosystems Research Facility, 1999.

APPENDIX A

A BRIEF SUMMARY OF POLYIMIDE FOLDABLE SUBSTRATE

In this section the details about the polyimide substrate is explained. There has been number of research in the polyimide substrate over the last decade. Polyimides are bio-compatible materials which has no harm when inserted into human body. The steps involved in polyimide substrate are as follows.

1. Formation of PDMS Cake

In order to have a polyimide substrate, it should be spin coated on a substrate which is hydrophobic in nature so that it can be peeled easily once the curing process is done. PDMS was chosen as the base substrate for polyimide coating. The PDMS is first mixed with the curing agent in the ratio 10:1 and kept in the vacuum for 15 minutes in order to remove the bubbles formed while mixing. Once the bubbles are removed, the PDMS is then poured into a dish and cured at 65^{o}C for 4 hours. Once the PDMS is cured, it is cut into 1"*1" pieces for further processing.

2. Treating with Oxygen Plasma

Since the PDMS is hydrophobic, the top surface is made hydrophilic by treating it with oxygen plasma for 10 minutes. The hydrophilic nature of PDMS lasts for only few hours and it is always better to start the subsequent spin coating process immediately following the oxygen plasma. Figure A.1 shows the cross section view of the PDMS cake.

Figure A.1: PDMS cake

3. Spin Coating Polyimide:

The next step is to spin coat polyimide, LTP 10-18A from the Fujifilm. The final spin speed is 2000 rpm and the thickness is approximately 6 µm. The soft bake temperature is 130^{o}C for 3 minutes. The total thickness required for mechanically stable substrate is about 20 µm and therefore multiple spin coating and baking was repeated. After the final spin coating, the polyimide can be peeled off from the PDMS cake easily.

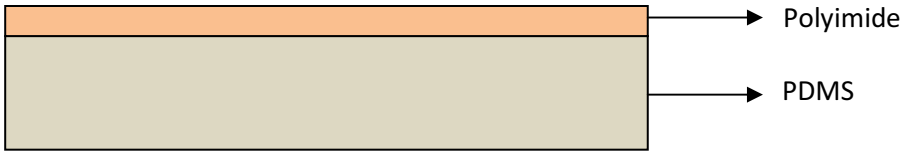

Figure A.2: Polyimide substrate on top of a PDMS cake

The initial idea was that the polyimide would curl itself while curing. The curing condition is at 200^{o}C for 1 hour. The cured polyimide was too strong enough to curl itself up. Figure A.3 shows the polyimide which has curled in random direction. It was difficult to control the curvature of the polyimide and figure A.4 shows the cured polyimide which is foldable and mechanically strong. The idea of sandwiching the polyimide around a thin layer of chromium and aluminum was tried in a hope that it can curl itself because of the difference in thermal expansion coefficient. The issue over here was that the metal layers were not deposited properly on top of

the polyimide due to the melting point of the polyimide in the deposition chamber. These issues have made us to discontinue the polyimide substrate and diverted towards silicon substrates.

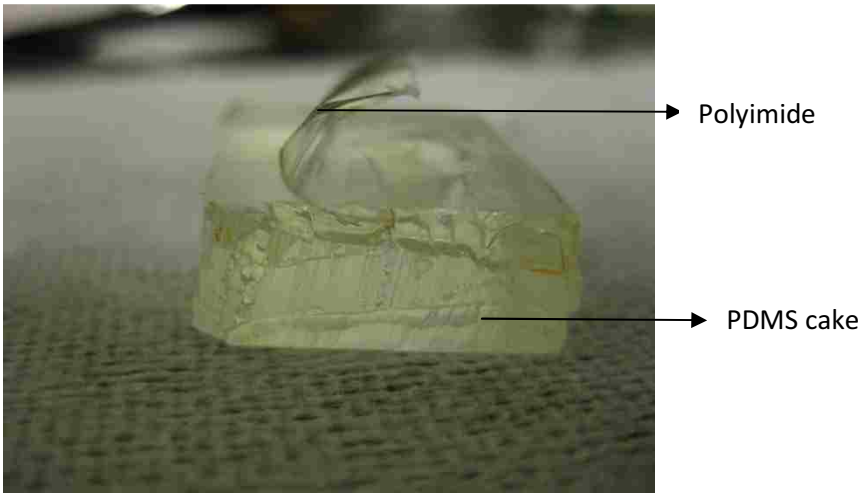

Figure A.3: PDMS cake and polyimide before curing

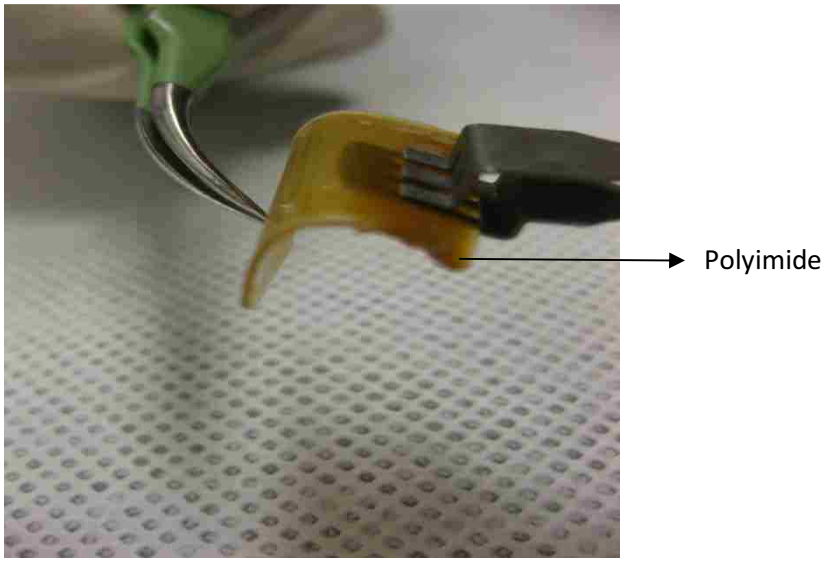

Figure A.4: Polyimide substrate after curing

APPENDIX B

SPIN COAT RECIPE FOR PHOTORESIST AND POLYIMIDE

1. AZ 9260 Photoresist

AZ 9260 is a positive photoresist from Microchemicals Inc. This is a thick photoresist and the final thickness of 15 µm can be easily achieved. Here in this thesis, the final thickness of 8 µm is used. The general recipe for obtaining 8 µm thickness is as follows.

Initial speed: 400 rpm for 5 seconds

Ramp: 800 rpm/sec

Intermediate speed: 1500 rpm for 20 seconds

Final speed: 2500 rpm for 50 seconds

Ramp: 1000 rpm/sec

2. Polyimide PI 5878G

PI 5878G is a thick non-photodefiniable polyimide from HD Microsystems. This polyimide requires the use of an adhesion promoter prior to spin coating. The adhesion promoter used is VM 651 from the same company. The spin coat recipe in order to obtain 3 µm thickness is as follows.

Initial speed: 500 rpm for 15 seconds

Ramp: 300 rpm/sec

Final speed: 5000 rpm for 60 seconds (intermediate spin speed is optional)

Ramp: 1200 rpm/sec

Dry spin: 400 rpm for 15 seconds

VITA

The author, Karthik Balasubramanian, was born in July 1986, in Salem, India. He graduated from S.S.B.M Matriculation Higher Secondary School, Salem, in May 2004. Beginning in August 2004, the author graduated from Anna University, Chennai, where he obtained Bachelor of Engineering degree in Electrical and Electronic Engineering in May 2008. He pursued his graduate studies in the department of Electrical and Computer Engineering at Louisiana State University (LSU) beginning August 2008 and obtained his Master of Science degree in December 2011.